NASA TECHNICAL NOTE

NASA TN D-4765

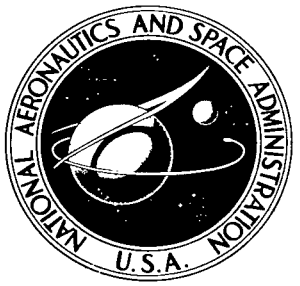

AN EXPLORATORY STUDY OF PARALLEL-STAGE SEPARATION OF REUSABLE LAUNCH VEHICLES

by John P. Decker and Joseph Gera

Langley Research Center
Langley Station, Hampton, Va.

NATIONAL AERONAUTICS AND SPACE ADMINISTRATION • WASHINGTON, D. C. • OCTOBER 1968

AN EXPLORATORY STUDY OF PARALLEL-STAGE SEPARATION OF REUSABLE LAUNCH VEHICLES

By John P. Decker and Joseph Gera

Langley Research Center
Langley Station, Hampton, Va.

NATIONAL AERONAUTICS AND SPACE ADMINISTRATION

For sale by the Clearinghouse for Federal Scientific and Technical Information
Springfield, Virginia 22151 – CFSTI price $3.00

AN EXPLORATORY STUDY OF PARALLEL-STAGE SEPARATION OF REUSABLE LAUNCH VEHICLES*

By John P. Decker and Joseph Gera
Langley Research Center

SUMMARY

An exploratory study has been made of the stage separation of parallel-staged reusable launch vehicles. Static longitudinal aerodynamic data were obtained for both stages of a representative two-stage rocket-powered reusable-launch-vehicle concept when the stages were in close proximity to each other. The effects of vertical spacing, longitudinal spacing, and incidence angle were determined at Mach numbers of 3 and 6. In an attempt to identify the problems associated with mutual stage interference during the separation maneuver, the equations of longitudinal motion were numerically integrated. The calculation was carried out for a limited number of initial conditions by using a portion of the wind-tunnel data along with estimated values of the dynamic derivatives.

The experimental results indicated large interference increments on the static-stability and normal-force characteristics of both vehicle stages. The static aerodynamic data for both vehicle stages were found to be dependent on the position and attitude of the second stage, the Mach number, and the relative sizes of the two stages. The relative sizes of the stages are dependent on the launch mode, the mission requirements, and the choice of propulsion system for the launch vehicle.

The trajectory results indicated a strong dependence of the dynamic derivatives, initial attitude, and dynamic pressure on the separation maneuver. These results also indicated that a potentially hazardous situation could be expected when parallel-arranged stages are separated. However, to evaluate the potential of safely separating any given system will require a critical staging analysis of the system under consideration to determine the constraints for which safe separation may be achievable. Furthermore, other avenues of approach, such as trajectory shaping, vehicle shaping, various thrusting maneuvers including attitude control thrust, stability augmentation, and other auxiliary devices need to be evaluated.

---

*The information presented herein was also presented in a thesis in partial fulfillment of the requirements for the degree of Master of Aerospace Engineering, University of Virginia, Charlottesville, Virginia, 1968.

INTRODUCTION

Interest in the potential of the recovery and reuse of launch vehicles during the past several years has resulted in a number of studies of various types of recoverable systems. The spectrum of concepts has varied from recoverable ballistic to winged reusable airbreathing vehicles. This paper is restricted to the class of reusable launch systems where the stages are arranged in parallel for launch. If staging must occur within the sensible atmosphere for these systems, aerodynamic interferences between the two vehicles may result in significant effects on the behavior of each vehicle during the staging maneuver. The Langley Research Center has therefore undertaken an exploratory investigation to ascertain these interferences and to interpret their influence on the staging maneuver. The discussion of reusable launch vehicles of reference 1 also indicated the existence of a potential problem in separating parallel-arranged stages of a reusable launch vehicle system. The present paper is an extension of the work presented in reference 2 and is an initial attempt to explore the complex problem of parallel-stage separation.

In order to provide meaningful information on the magnitude and character of the staging problem, it is necessary to obtain aerodynamic test data on each of the two vehicles in close proximity at conditions which might occur during staging and then to estimate the effects of these forces and moments on the relative motion of the two vehicles. For the present investigation, which is primarily exploratory, static longitudinal data were obtained on two representative stages of a rocket-powered reusable-launch-vehicle system when the vehicles were in close proximity to each other to obtain some understanding of the aerodynamic-interference phenomena. The first stage was a simplified wing-body configuration whereas the second stage was a lifting body. Vertical and longitudinal spacing, as well as incidence angle, were varied for a range of angle of attack and at Mach numbers of 3 and 6. These data were then used in integrating the equations of motion of both vehicles to determine the relative behavior of both stages during a staging maneuver. This analysis was made by using the coupled longitudinal equations of motion for both stages. In these equations, the general load terms were replaced by the experimental aerodynamic data and estimates of the damping derivatives. For selected values of stage characteristics and initial conditions, the equations were solved numerically.

SYMBOLS

The aerodynamic loads of each stage have been resolved and reduced into coefficient form with respect to its own body-axis system. The location of the origin, and the orientation of the body axes are shown for the two body-axis systems in figure 1. The geometric constants used in reducing the aerodynamic loads into coefficient form are

given in table I. The physical quantities defined in this paper are given in both the U.S. Customary System of Units and the International System of Units (SI). Conversion factors between the two systems are given in reference 3.

A planform area of second-stage pitch control flaps, feet^2 (meters^2)

C_A axial-force coefficient, $\frac{\text{Measured axial force}}{\frac{k}{2}pM^2S}$

C_m pitching-moment coefficient, $\frac{\text{Measured pitching moment}}{\frac{k}{2}pM^2Sc}$

C_{m_q} damping in pitch, $\frac{\partial C_m}{\partial \frac{qc}{2V}}$

$C_{m_{\dot{w}}}$ rate of change of pitching moment due to acceleration along Z-axis, $\frac{\partial C_m}{\partial \dot{w}}$, seconds^2/foot (seconds^2/meter)

C_N normal-force coefficient, $\frac{\text{Measured normal force}}{\frac{k}{2}pM^2S}$

C_{N_q} rotary stability derivative, $\frac{\partial C_N}{\partial \frac{qc}{2V}}$

C_{N_α} normal-force slope, $\frac{\partial C_N}{\partial \alpha}$, per degree

C_T thrust coefficient, $\frac{\text{Thrust force}}{\frac{k}{2}pM^2S}$

c reference length (see table I); for the first stage it is equal to the mean aerodynamic chord, for the second stage it denotes the body length, feet (meters)

d distance between centers of mass, feet (meters)

d_T perpendicular distance from center of mass to line of thrust, feet (meters)

F_X, F_Z components of resultant force, pounds (newtons)

g acceleration due to gravity, feet/second^2 (meters/second^2)

h altitude, $-z_e$, feet (meters)

I_Y	mass moment of inertia, slug-feet^2 (kilogram-meters^2)
i	incidence angle, $\alpha_2 - \alpha_1$, degrees
k	ratio of specific heats
l	body length, feet (meters)
M	Mach number
M_Y	total pitching moment, foot-pounds (meter-newtons)
m	mass, slugs (kilograms)
p	static pressure, pounds/foot^2 (newtons/meter^2)
q	angular velocity, radians/second
R	radius, inches (centimeters)
S	reference area (see table I), feet^2 (meters^2)
t	time, seconds
u,w	components of velocity along body axes, feet/second (meters/second)
V	resultant velocity, $\left(u^2 + w^2\right)^{1/2}$, feet/second (meters/second)
X,Y,Z	coordinate axes
x,z	distances along body axes, feet (meters)
x_e,z_e	distances along earth-fixed axes, feet (meters)
x_a,x_b,r_a,z_a	fuselage coordinates (see fig. 1(b)), inches (centimeters)
$\Delta x,\Delta z$	separation variables (positive when center of gravity of second stage is ahead and above center of gravity of first stage, see fig. 4), feet (meters)
α	angle of attack, degrees

γ flight-path angle, $\theta - \alpha$, degrees

δ_e resultant angle of pitch control flap (positive when trailing edge is down), $\frac{\delta_{e,right} + \delta_{e,left}}{2}$, degrees

ϵ angle between X-axis and thrust line, degrees

θ angle of pitch, degrees

ρ atmospheric density, slugs/foot^3 (kilograms/meter^3)

Δt time increment, seconds

A dot over a symbol denotes first derivative with respect to time.

The subscripts 1 and 2 indicate whether the physical quantity represented by the principal symbol refers to stage 1 or stage 2.

APPARATUS AND TESTS

Models

Details of the launch-vehicle configuration are shown in figure 1. The launch vehicle consisted of a simplified wing-body first stage with a lifting-body second stage. The second stage was placed on top of the first stage, the flat bottom being parallel with the first-stage wing upper surface. The longitudinal location of the second stage was such that its moment reference center was behind the first-stage moment reference center in the normal carrying position, that is, $\Delta x/l_1 = -0.051$. Photographs of the two-stage system prior to staging and at staging conditions are shown in figure 2.

The first stage consisted of a semicylindrical fuselage with an ogival forebody and delta wing. The wing had 65° leading-edge sweep and the airfoil section was a half-diamond section that had a maximum thickness of 4 percent of the local chord at the 40-percent-chord station. The wing was flat on the upper surface, and thus the wing had negative camber. No longitudinal or vertical control surfaces were provided on the first stage for the present tests.

The second stage was a lifting-body type of vehicle with cross-sectional shape progressions along the X-axis as shown in figure 1(c). The second stage had essentially a flat bottom and was provided with vertical stabilizing surfaces. Pitch controls were provided on the second stage which consisted of upper and lower surface flaps located near

the base of the body. (See fig. 1(c).) The ratio of planform area of the pitch controls to the total planform area was 0.113 for the upper surface controls and 0.187 for the lower surface controls.

Support Mechanism

Separate sting supports were provided for the first and second stage, preset vertical movement between the stages being provided in the vertical plane by the support system to which the stings were attached. (See fig. 3.) Longitudinal movement and incidence angle between the stages were provided by using spacers and sting adapters on the upper sting support. The complete support apparatus was attached to an arc strut which varied the angle of attack of the vehicles.

Tests

The wind-tunnel tests were conducted at nominal Mach numbers of 3 and 6 in the 2-foot hypersonic facility at the Langley Research Center described in reference 4. Position variables Δx and Δz, as well as the relative incidence angle i, were varied for an angle-of-attack range of approximately -9° to 12°. (See fig. 4.) Static longitudinal aerodynamic force and moment data were simultaneously obtained for the first and second stage by use of individual internal six-component strain-gage balances. No composite configurations, that is, with the first stage and second stage connected, were tested.

All data were obtained with the model smooth; that is, no boundary-layer transition strips were used. At the Reynolds numbers of these tests, laminar flow may be expected to exist over most of the model. Individual vehicle angles of attack were corrected for balance and sting deflection under load. No base drag corrections were made for either the first or second stage. The average tests conditions and Reynolds number variations are as follows:

Mach number	Stagnation pressure		Stagnation temperature		Reynolds number based on a 1-foot (0.3048 m) length
	atm	kN/m^2	$^{\circ}R$	$^{\circ}K$	
3	0.5	50.6	560	322	0.8×10^6
6	3.0	303.6	760	422	1.0

METHOD OF ANALYSIS

The separation maneuver of two parallel stages is illustrated schematically in figure 5. At release, the second stage would be at an initial spacing distance and attitude

with respect to the first stage. A trapeze or similar mechanism could be employed to achieve the desired release conditions. Potential problems that may arise during the staging sequence are illustrated by the lower two sketches of figure 5. The divergence of the center of gravity alone would not imply safe separation since the second stage may rotate into the first stage. Consequently, realistic analysis can only be accomplished if the separation maneuver is regarded as the motion of rigid bodies.

Two parallel lifting stages, separating from each other aerodynamically, represent a complex dynamic system. For the complete description of this system, not less than 12 degrees of freedom must be taken into account. Although this is possible, at least theoretically, the final accuracy of the analysis will depend on the correct analytical representation of the aerodynamic forces and moments.

From the available data, the aerodynamic loads cannot be predicted if any lateral motion occurs during the separation maneuver; therefore, it is assumed that the motion of both stages takes place in the common plane of symmetry. With this restriction, the Euler equations of motion (ref. 5) with respect to the body axes for either stage are

$$\left.\begin{aligned} m(\dot{u} + wq) &= F_X - mg \sin\theta \\ m(\dot{w} - uq) &= F_Z + mg \cos\theta \\ I_Y\dot{q} &= M_Y \end{aligned}\right\} \tag{1}$$

The angular orientation and position of either stage are expressed as

$$\left.\begin{aligned} \dot{\theta} &= q \\ \dot{x}_e &= u \cos\theta + w \sin\theta \\ \dot{z}_e &= -u \sin\theta + w \cos\theta \end{aligned}\right\} \tag{2}$$

This set of six equations is completely general and valid even for large disturbances. However, in the development of the expressions for the force and moment terms, the following assumptions are made:

(1) Since the time lapse between the initiation of the separation maneuver and full separation (or collision) of the two stages is small, the response of the system to any control deflection is assumed to be negligible. Hence, the controls are considered to be fixed.

(2) During separation, the effects of speed changes on the aerodynamic-force coefficients are neglected.

(3) Cross coupling between the two stages takes place only through the normal-force and pitching-moment coefficients. Consequently, the axial-force coefficient of either stage was assumed not to be affected by the proximity of the other stage.

With these assumptions, the force and moment terms may be expressed as

$$\left.\begin{aligned} F_X &= \tfrac{1}{2}\rho V^2 S\left(C_T \cos \epsilon - C_A\right) \\ F_Z &= \tfrac{1}{2}\rho V^2 S\left(C_T \sin \epsilon - C_N + \frac{c}{2V} C_{N_q} q\right) \\ M_Y &= \tfrac{1}{2}\rho V^2 Sc\left(\frac{d_T}{c} C_T + C_m + \frac{c}{2V} C_{m_q} q + C_{m_{\dot{w}}} \dot{w}\right) \end{aligned}\right\} \tag{3}$$

In equations (3) the rotary stability derivatives C_{N_q} and C_{m_q} and the derivative $C_{m_{\dot{w}}}$ are considered to be constants for each stage during the separation maneuver since these derivatives are not presently available for two vehicles in close proximity. However, the influence of these derivatives on the separation maneuver can be investigated by varying the magnitude of these quantities. Orientation of the thrust vector is specified by ϵ (the angle between the X-axis and the thrust vector) and d_T (the perpendicular distance from the center of gravity to the thrust line). These quantities, as well as the thrust coefficient C_T, were assumed to be constant for each stage since the time lapse between the initiation of the separation maneuver and full separation (or collision) of the two stages is small. Equations (3) are arbitrary to a large extent, and they were written with the experimental part of this investigation in mind. The aerodynamic coefficients, C_A, C_N, and C_m, represent the experimental data measured on each stage.

Up to this point, the form of the governing equations has been identical for both stages. For each stage, however, the aerodynamic coefficients are defined separately, that is,

$$\left.\begin{aligned} C_{A,1} &= C_{A,1}(\alpha_1) \\ C_{A,2} &= C_{A,2}(\alpha_1) \\ C_{N,1} &= C_{N,1}(\alpha_1,\alpha_2,\Delta x,\Delta z) \\ C_{N,2} &= C_{N,2}(\alpha_1,\alpha_2,\Delta x,\Delta z) \\ C_{m,1} &= C_{m,1}(\alpha_1,\alpha_2,\Delta x,\Delta z) \\ C_{m,2} &= C_{m,2}(\alpha_1,\alpha_2,\Delta x,\Delta z) \end{aligned}\right\} \tag{4}$$

From the experimental data of the present investigation, these relations can be constructed explicitly in the form of tabular functions. The separation variables, α_1, α_2, Δx, and Δz, are illustrated in figure 4.

The resulting equations of motion were integrated numerically on a digital computer. The values of the aerodynamic coefficients were obtained by linear interpolation between the discrete points of the tabular functions at each integration step. The

atmospheric density ρ in equations (3) corresponds to that given by the U.S. Standard Atmosphere, 1962 (ref. 6) at each height.

For the numerical integration, the size of the computing interval was carefully selected by the use of two different integration techniques for each of which the size of the computing interval was systematically varied. Comparison of the solutions obtained in this manner indicated that a value of Δt between the values of 0.005 and 0.01 second resulted in an acceptable level of accuracy. Consequently, a fourth-order fixed-interval integration technique was used. This integration technique uses the Adams-Bashforth predictor formula in conjunction with the Adams-Moulton correction formula. A fourth order Runge-Kutta formula with minimum error bounds was used to start the solution. (See refs. 7 and 8.) The integration did not proceed beyond $t = 5$ seconds since safe separation or collision occurred within this time.

When the numerical solutions of the present analysis are interpreted, it should be remembered that in addition to the assumptions listed, equations (3) contain another source of potential error. Ideally, the unaccelerated flight of a single body can be completely simulated in the wind tunnel, whereas the separating flight of two parallel stages is impossible to simulate either kinematically or dynamically with fixed models in the test section. Thus, the direct use of the measured coefficients in equations (3) involves the error due to the wind-tunnel simulation technique where the coefficient data could be obtained only at $\gamma_1 = \gamma_2$ and $V_1 = V_2$. This error is lessened by using the magnitudes of the instantaneous velocities in equations (3). However, this procedure will not take into account the effects of different flight-path angles on the aerodynamic interference nor any scaling or Reynolds number effects.

PRESENTATION OF RESULTS

The results have been divided into two principal parts. These two parts consist of the experimental results obtained for the two stages in close proximity and the calculated results obtained by integrating the equations of motion for each of the two stages during a staging maneuver. Since the aerodynamic interferences that occur when two bodies are in close proximity are potential stability and control problems for both vehicle stages, the experimental results are used to discuss the implication of these interferences on the stability characteristics of the stages when in close proximity, whereas the calculated results are used to discuss the potential effects on the vehicle behavior of the aerodynamic interference.

EXPERIMENTAL RESULTS

The basic longitudinal aerodynamic characteristics of the first and second stages at different vertical and longitudinal spacings, incidence angles, and Mach numbers are presented in figures 6 to 9. For reference, the interference-free data, or the data at a very large separation distance $\left(\Delta z/l_1 = \infty\right)$, are also shown in these figures.

First Stage

Second-stage moment reference center aft of first-stage moment reference center; $\Delta x/l_1 = -0.051$.- Figure 6(a) presents the effect of vertical spacing at $M = 3$, $i = 0^o$, second-stage moment reference center aft of first-stage moment reference center, and $\Delta x/l_1 = -0.051$. This figure indicates that the static stability level did not change appreciably with vertical spacing. However, there is a large positive increment in $C_{m,1}$ due to the interference and a significant change in the angle for trim. Also, for the maximum vertical spacing of the tests, large interferences are still present because the curve at $\Delta z/l_1 = 0.224$ has not approached the interference-free curve $\left(\Delta z/l_1 = \infty\right)$. Figure 6(a) also shows that there are large negative increments in $C_{N,1}$ due to the interference and no appreciable change in $\left(C_{N_\alpha}\right)_1$. Increasing i from 0^o to 5^o (fig. 6(b)) and 10^o (fig. 6(c)) at $M = 3$ resulted in further positive increments in $C_{m,1}$ and further negative increments in $C_{N,1}$. (Compare $C_{m,1}$ and $C_{N,1}$ at $\Delta z/l_1 = 0.127$, for example.)

At $M = 6$ and $i = 0^o$, figure 7(a) shows that both the magnitude of $C_{m,1}$ and stability level of the first stage varied with vertical spacing. This result is in contrast to the data at $M = 3$ (fig. 6(a)) where only the magnitude of $C_{m,1}$ was shown to vary with vertical spacing. Also in contrast to the data at $M = 3$, the data at the largest vertical spacing $\left(\Delta z/l_1 = 0.224\right)$ at $M = 6$ (fig. 7(a)) indicates that the first stage is approaching interference-free conditions since both the normal-force and pitching-moment curves are approaching the interference-free curves. However, at this vertical spacing and also at $\Delta z/l_1 = 0.199$, the first stage has pitch-up tendencies at α_1 greater than 3^o. Increasing i from 0^o to 10^o (figs. 7(a), 7(b), and 7(c)) at $M = 6$ caused positive increments in $C_{m,1}$ and a degradation of the static stability at all vertical spacings. Figures 7(a), 7(b), and 7(c) also show that the presence of the second stage caused negative increments in $C_{N,1}$ and some localized changes in $\left(C_{N_\alpha}\right)_1$ as compared with interference-free conditions.

Second-stage moment reference center forward of first-stage moment reference center; $\Delta x/l_1 = 0.160$.- At the forward longitudinal spacing $\Delta x/l_1 = 0.160$ and at $M = 3$ and $i = 0^o$ (fig. 6(d)) not only did the magnitude of $C_{m,1}$ vary with vertical spacing, but also the stability level decreased with increasing vertical spacing so that at $\Delta z/l_1 = 0.199$ and 0.244, the first stage is statically unstable at α_1 less than about 2^o.

Figure 6(d) also shows that in comparison with the interference-free curve, both $(C_{N_\alpha})_1$ and the magnitude of $C_{N,1}$ at α_1 greater than about -8° decreased because of the presence of the second stage. However, increasing the vertical spacing did not appreciably change either $(C_{N_\alpha})_1$ or $C_{N,1}$. Increasing i from 0° to 10° (figs. 6(d), 6(e), and 6(f)) caused further decreases in the stability level, the magnitude of $C_{m,1}$, and the magnitude of $C_{N,1}$, as compared with the interference-free curves.

At M = 6 (figs. 7(d), 7(e), and 7(f)), the first stage was statically unstable at the smaller vertical spacings for α_1 less than about 2°. These same figures also show that the magnitude of $C_{m,1}$, $C_{N,1}$, and $(C_{N_\alpha})_1$ varied with vertical spacing.

Second Stage

Second-stage moment reference center aft of first-stage moment reference center; $\Delta x/l_1 = -0.051$.- For the second stage at M = 3, i = 0°, second-stage moment reference center aft of first-stage moment reference center, and $\Delta x/l_1 = 0.051$ (fig. 8(a)), both the stability level and magnitude of $C_{m,1}$ varied with vertical spacing. At $\Delta z/l_1$ less than 0.175, the second stage was approximately neutrally stable or statically unstable at all α_1. Coupled with these changes in stability and magnitude of $C_{m,2}$ are changes in both $C_{N,2}$ and $(C_{N_\alpha})_2$. Increasing i from 0° to 10° at M = 3 (figs. 8(a), 8(b), and 8(c)) caused the second-stage stability level to decrease and caused large negative increments in the magnitude of $C_{m,2}$ and large positive increments in $C_{N,2}$. Comparison of the normal-force and pitching-moment data (figs. 8(a), 8(b), and 8(c)) with the corresponding data for the first stage (figs. 6(a), 6(b), and 6(c)) indicates that increasing i would tend to cause the first stage to nose up but away $(-C_{N,1})$ from the second stage, whereas the second stage would tend to nose down but away $(+C_{N,2})$ from the first stage.

Comparison of the data for the second stage at M = 3 (figs. 8(a), 8(b), and 8(c)) with the data at M = 6 (figs. 9(a), 9(b), and 9(c)) at similar geometric conditions indicates that the results at both Mach numbers are very similar. As would be expected, increasing the Mach number from 3 to 6 decreased the actual magnitude of the force and moment coefficients.

Second-stage moment reference center forward of first-stage moment reference center; $\Delta x/l_1 = 0.160$.- At M = 3, second-stage moment reference center forward of first-stage moment reference center and $\Delta x/l_1 = 0.160$, figures 8(d), 8(e), and 8(f) indicate that the second stage was statically stable at almost all vertical spacings, incidence angles, and α_1. However, the presence of the first stage caused increments in both $C_{m,2}$ and $C_{N,2}$, the increments becoming larger with increasing i. Again, similar results are shown at M = 6. (See figs. 9(d), 9(e), and 9(f).)

Second-stage control effectiveness.- Because of the large interference increments found for the second stage, an investigation was made to determine the control effectiveness of the second stage at interference-free conditions. Figure 10 presents this control effectiveness data for control deflections of 0^{o} and $\pm 25^{o}$. Comparison of these data with the data in figures 8 and 9 indicates that there appears to be no reasonable control deflection which could overcome all the large pitching-moment increments shown for the second stage when in proximity to the first stage.

Comments on Interference Increments

Further analysis of the data shown in figures 6 to 9, along with schlieren data, has led to two major conclusions as to the source of the behavior of the force and moment coefficients as compared with the interference-free values. These conclusions are illustrated in figure 11. The first conclusion is that the effects on the first stage are caused by the impingement of the principal disturbance generated by the second stage. Consequently, the changes in forces and moments previously shown for the first stage are approximately proportional to the strength of this disturbance and the area affected. The second conclusion is that the effects on the second stage are caused by the flow field from the first stage to which must be added the effects of the first reflection of the principal disturbance caused by the second stage. Furthermore, not only are the static aerodynamic data dependent on the relative position and attitude of the second stage and Mach number, but the data are also dependent on the relative sizes of the two stages since the flow field of the first stage and the strength of the disturbance generated by the second stage are a direct function of the sizes of the two vehicles. The relative sizes of the two stages are dependent on the launch mode, the mission requirement, and the choice of propulsion system for the launch vehicle.

TRAJECTORY RESULTS

The time involved in obtaining solutions of the equations of motion (eqs. (1) and (2)) for each stage put practical limits on the number of variables and vehicle characteristics investigated. Accordingly, staging was assumed to occur in climbing flight and the Mach number selected for the analysis was 3 since this value could correspond to either an abort or mission-staging condition. These considerations led to the selection of a number of fixed vehicle characteristics and initial conditions given in table II.

Presented in figure 12 is a typical altitude Mach number ascent trajectory plot shown only out to a Mach number of 8 and indicates where abort and mission-staging conditions might be required. Reusable launch vehicles using airbreathing engines may stage at the lower altitudes and consequently higher dynamic pressures whereas rocket-powered vehicles would stage at the higher altitudes and lower dynamic pressures.

Reference 1 has indicated that airbreathing vehicles may be able to stage at the lower dynamic pressures with a negligible performance decrement by executing a pull-up maneuver. Normal mission staging could occur, depending on the vehicle concept, anywhere above a Mach number of about 3, whereas abort staging could occur at any Mach number below mission staging and at any altitude.

Example Solutions

Figure 13 illustrates typical numerical results at an altitude of 70 000 feet (21 336 meters) for two particular choices of the initial conditions and the damping-in-pitch characteristics. The vehicles were assumed to have safely separated when the vehicles were one first-stage body length apart and were assumed to have collided when the extremities of the vehicles touched each other. The main points of this figure are that (1) the time it took the vehicles to collide or separate was of the order of 3 seconds, a very short time for aerodynamic controls to be effective; (2) the net change in the initial and final velocities of either stage during the separation maneuver would amount to a net Mach number change of about 0.10 and would have a negligible effect on the static aerodynamic coefficients; and (3) the difference between γ_1 and γ_2 which was a maximum of 1.75° for the safe separation case, could introduce some errors in the calculations since the static aerodynamic coefficients were obtained for $\gamma_1 = \gamma_2$ and could affect whether the vehicles would collide or safely separate.

As was previously implied, no attempt was made in the present study to investigate the effect of all important vehicle characteristics, initial conditions, and damping characteristics either separately or in all reasonable combinations. Instead, attention was given to some of the least accurately estimated damping variables, namely, $(C_{mq})_1$ and $(C_{mq})_2$, and to some of the initial conditions which have obvious bearing on successful separation. Included in the latter category were the initial relative attitude, dynamic pressure, and vertical thrusting.

Effect of Dynamic Derivatives

Figure 14 shows the effect of the dynamic derivatives where $(C_{mq})_1$ is plotted against $(C_{mq})_2$. Indicated in this figure are the regions where the two vehicles collided, an approximate region where they safely separated, and a region of uncertainty as to whether the two vehicles would collide or separate. Also indicated in this figure are the best current estimates of the interference-free values of C_{mq} for both the first and second stages. These values are one or more orders of magnitude smaller than the values needed to achieve safe separation at these conditions. Although the magnitude of $C_{m_{\dot{w}}}$ and C_{Nq} for both the first and second stages have not been perturbed in this analysis, it can be expected that similar figures would be generated for these quantities.

Effect of Initial Attitude

For the purpose of illustrating some of the other important variables that may need to be considered to achieve safe separation, figure 15 shows the type of results that can be generated by selecting a value of C_{m_q} which lies in the safe separation region for both the first and second stages (square symbol, fig. 14). Here the incidence angle and the angle of attack of the first stage have been varied. Again, the regions of collision and safe separation are shown.

Effect of Dynamic Pressure

Figure 16 shows the effect of varying the dynamic pressure or altitude for the separation maneuver by taking a suitable safe separation value of i and α_1 (circular symbol, fig. 15). The distance between the centers of gravity of the two stages in 2 seconds after release has been plotted against dynamic pressure. The dynamic-pressure range is for altitudes above and below the nominal altitude for a rocket-powered vehicle at $M = 3$. Two curves are presented; one is for the condition in which no thrust was used in the calculations and the other is for the condition in which a hypothetical vertical downward thrust corresponding to a thrust-weight ratio of 0.1 has been applied to the first stage. Using either vertical or longitudinal thrust would present jet-plume body interactions which, in these calculations, have not been evaluated. For the no-thrust condition and at zero dynamic pressure, the position and attitude of the vehicles do not change; and separation does not occur. Safe separation can be expected only at the higher dynamic pressures for the no-thrust condition. For the vertical-thrust condition, safe separation could result at low dynamic pressures but as the dynamic pressure increases, there is a region of collision. At the higher dynamic pressures, safe separation would also be predicted.

Figures 14, 15, and 16 have indicated some of the problems associated with parallel-stage separation. These results have indicated that evaluating the potential of any parallel-staged system requires a critical dynamic analysis of the two vehicles when in close proximity to determine the constraints under which safe separation of the two vehicles may be achievable.

CONCLUDING REMARKS

An exploratory study has been made of the stage separation of parallel-staged reusable launch vehicles. Static longitudinal aerodynamic data were obtained for both stages of a representative two-stage rocket-powered reusable-launch-vehicle concept when the stages were in close proximity to each other. The effects of vertical spacing, longitudinal spacing, and incidence angle were determined at Mach numbers of 3 and 6.

In an attempt to identify the problems associated with mutual stage interference during the separation maneuver, the equations of longitudinal motion were numerically integrated. The calculation was carried out for a limited number of initial conditions by using a portion of the wind-tunnel data along with estimated values of the dynamic derivatives.

The experimental results indicated large interference increments on the static-stability and normal-force characteristics of both vehicle stages. The static aerodynamic data for both vehicle stages were found to be dependent on the position and attitude of the second stage, the Mach number, and the relative sizes of the two stages. The relative sizes of the stages are dependent on the launch mode, the mission requirements, and the choice of propulsion system for the launch vehicle.

The trajectory results indicated a strong dependence of the dynamic derivatives, initial attitude, and dynamic pressure on the separation maneuver. These results also indicated that a potentially hazardous situation could be expected in separating parallel-arranged stages. However, to evaluate the potential of safely separating any given system will require a critical staging analysis of the system under consideration to determine the constraints for which safe separation may be achievable. Furthermore, other avenues of approach, such as trajectory shaping, vehicle shaping, various thrusting maneuvers including attitude control thrust, stability augmentation, and other auxiliary devices need to be evaluated.

Langley Research Center,
National Aeronautics and Space Administration,
Langley Station, Hampton, Va., April 17, 1968,
124-07-05-02-23.

REFERENCES

1. Petersen, Richard H.; Gregory, Thomas J.; and Smith, Cynthia L.: Some Comparisons of Turboramjet-Powered Hypersonic Aircraft for Cruise and Boost Missions. J. Aircraft, vol. 3, no. 5, Sept.-Oct. 1966, pp. 398-405.

2. Decker, John P.: Experimental Aerodynamics and Analysis of the Stage Separation of Reusable Launch Vehicles. Conference on Hypersonic Aircraft Technology. NASA SP-148, 1967, pp. 63-77.

3. Mechtly, E. A.: The International System of Units – Physical Constants and Conversion Factors. NASA SP-7012, 1964.

4. Stokes, George M.: Description of a 2-Foot Hypersonic Facility at the Langley Research Center. NASA TN D-939, 1961.

5. Babister, A. W.: Aircraft Stability and Control. Pergamon Press, c.1961.

6. Anon.: U.S. Standard Atmosphere, 1962. NASA, U.S. Air Force, and U.S. Weather Bur., Dec. 1962.

7. Henrici, Peter: Discrete Variable Methods in Ordinary Differential Equations. John Wiley & Sons, Inc., c.1962.

8. Ralston, Anthony: Runge-Kutta Methods With Minimum Error Bounds. Mathematics of Computation, vol. 16, no. 80, Oct. 1962, pp. 431-437.

TABLE I.- GEOMETRIC CHARACTERISTICS OF MODELS AND REFERENCE DIMENSIONS

First stage:		
Body length, in. (cm)	23.760	(60.350)
Overall length, in. (cm)	23.760	(60.350)
Aspect ratio	1.865	
Span, in. (cm)	13.802	(35.057)
Total wing area, in^2 (cm^2)	102.135	(658.934)
Reference area, in^2 (cm^2)	102.135	(658.934)
Root chord, in. (cm)	14.800	(37.592)
Tip chord	0	
Mean aerodynamic chord, in. (cm)	9.867	(25.062)
Reference length, in. (cm)	9.867	(25.062)
Second stage:		
Body length, in. (cm)	11.465	(29.121)
Overall length, in. (cm)	13.706	(34.813)
Aspect ratio	0.678	
Span, in. (cm)	6.050	(15.367)
Planform area less vertical fins, in^2 (cm^2)	53.980	(348.257)
Reference area, in^2 (cm^2)	53.980	(348.257)
Reference length, in. (cm)	11.465	(29.121)

TABLE II.- VEHICLE CHARACTERISTICS AND INITIAL CONDITIONS

First stage:	
Weight, lb (N)	345 000 (1 534 636)
I_Y, slugs-ft^2 (kg-m^2)	11.00×10^6 (14.9×10^6)
c, ft (m)	78.11 (23.81)
S, ft^2 (m^2)	6401 (594.7)
$C_{m_{\dot{w}}}$, sec^2/ft (sec^2/m)	-0.00002 (-0.00006)
C_{m_q}	Variable
C_{N_q}	0
V_1, ft/sec (m/sec)	3100 (945)
γ_1, deg	26
l_1, ft (m)	188.1 (57.33)
Second stage:	
Weight, lb (N)	300 000 (1 347 811)
I_Y, slugs-ft^2 (kg-m^2)	1.75×10^6 (2.4×10^6)
c, ft (m)	90.76 (27.66)
S, ft^2 (m^2)	3383 (314.3)
$C_{m_{\dot{w}}}$, sec^2/ft (sec^2/m)	-0.000005 (-0.00001)
C_{m_q}	Variable
C_{N_q}	0
$\Delta x/l_1$	-0.051
$\Delta z/l_1$	0.127
γ_2, deg	26
V_1, ft/sec (m/sec)	3100 (945)

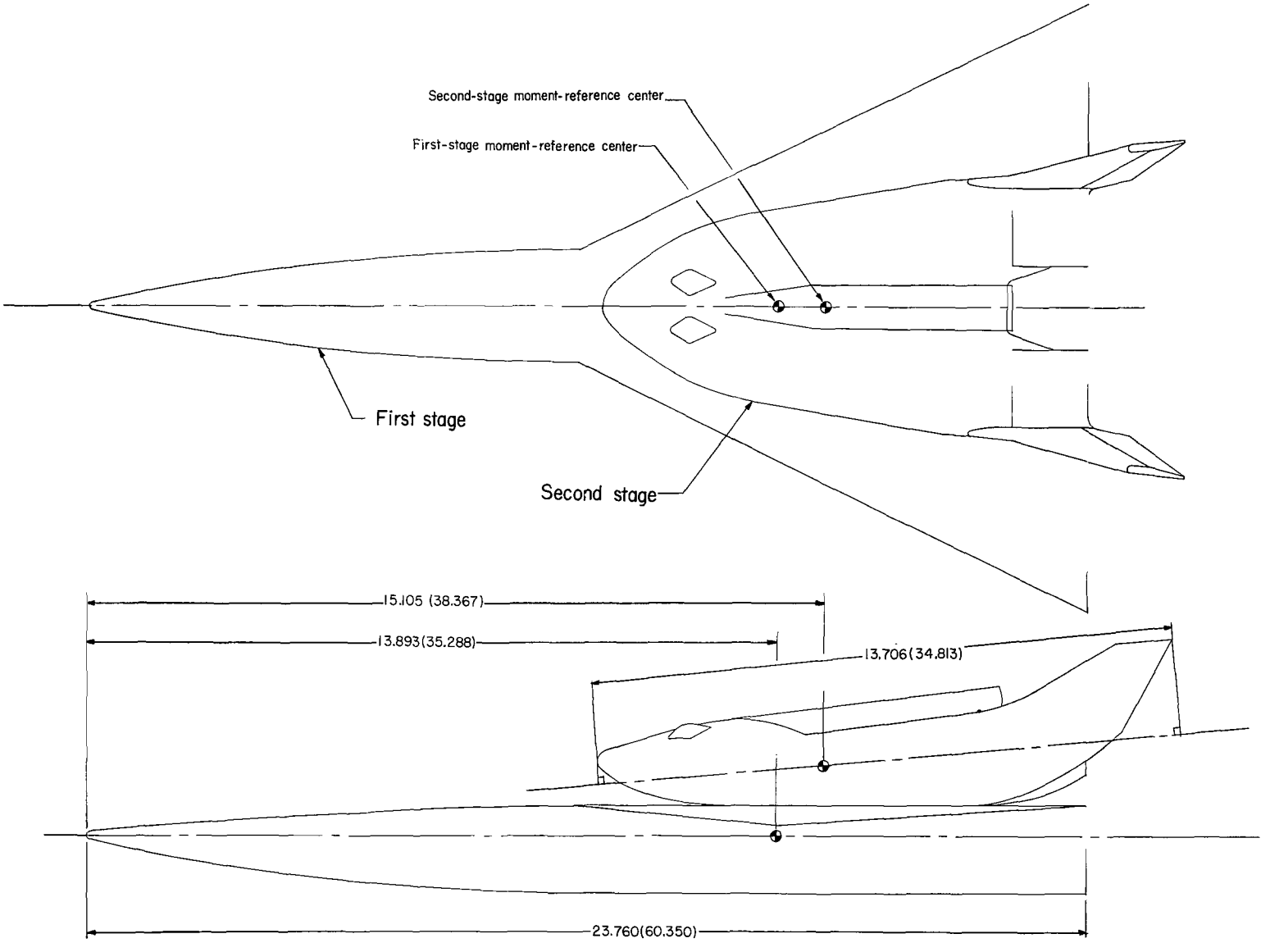

(a) Launch vehicle.

Figure 1.- Details of models. (All dimensions are given in inches, parenthetically in centimeters.)

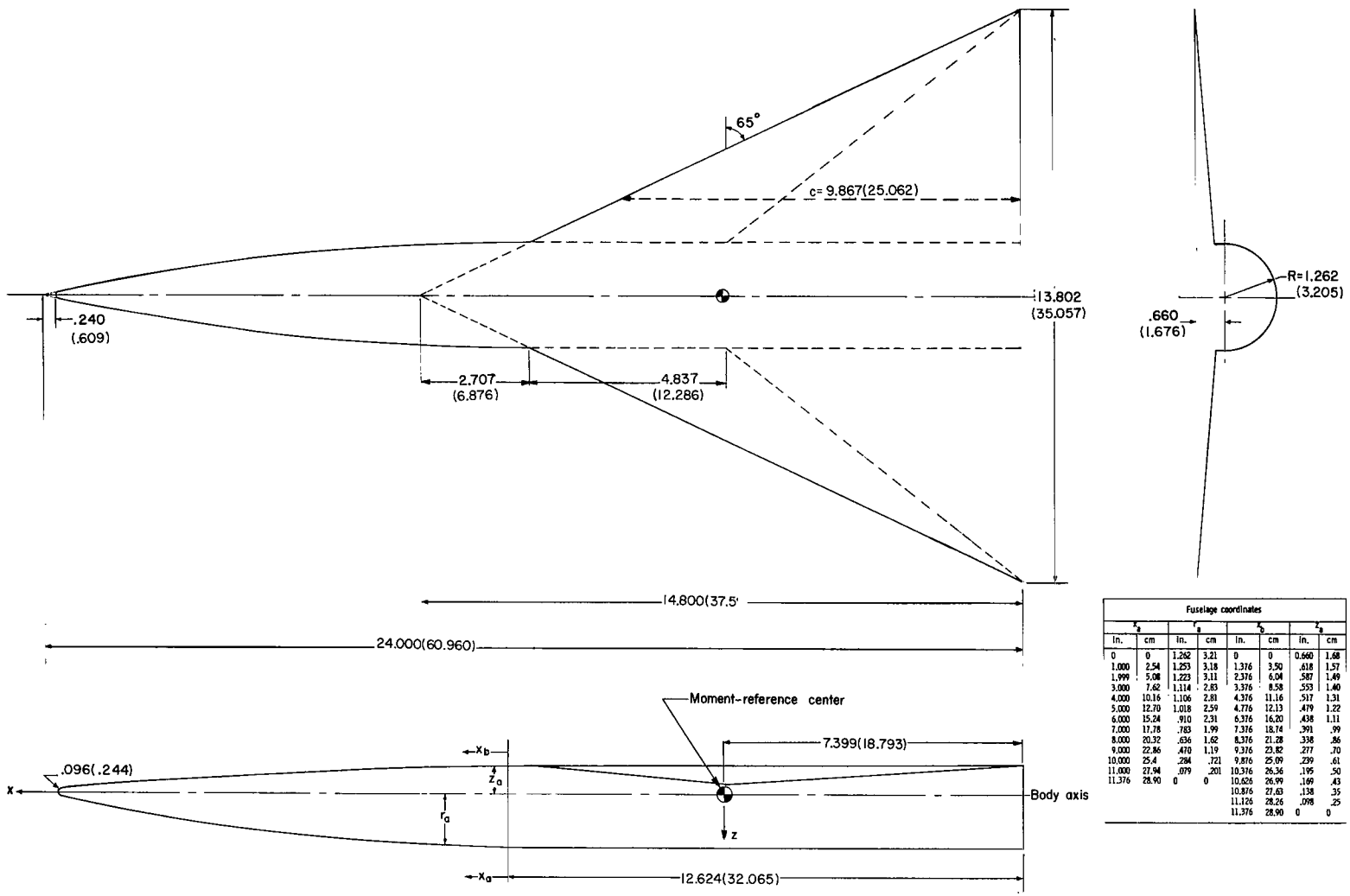

Fuselage coordinates

z_a		r_a		x_b		z_a	
in.	cm	in.	cm	in.	cm	in.	cm
0	0	1.262	3.21	0	0	0.660	1.68
1.000	2.54	1.253	3.18	1.376	3.50	.618	1.57
1.999	5.08	1.223	3.11	2.376	6.04	.587	1.49
3.000	7.62	1.114	2.83	3.376	8.58	.553	1.40
4.000	10.16	1.106	2.81	4.376	11.16	.517	1.31
5.000	12.70	1.018	2.59	4.776	12.13	.479	1.22
6.000	15.24	.910	2.31	6.376	16.20	.438	1.11
7.000	17.78	.783	1.99	7.376	18.74	.391	.99
8.000	20.32	.636	1.62	8.376	21.28	.338	.86
9.000	22.86	.470	1.19	9.376	23.82	.277	.70
10.000	25.4	.284	.721	9.876	25.09	.239	.61
11.000	27.94	.079	.201	10.376	26.36	.195	.50
11.376	28.90	0	0	10.626	26.99	.169	.43
				10.876	27.63	.138	.35
				11.126	28.26	.098	.25
				11.376	28.90	0	0

(b) First stage.

Figure 1.- Continued.

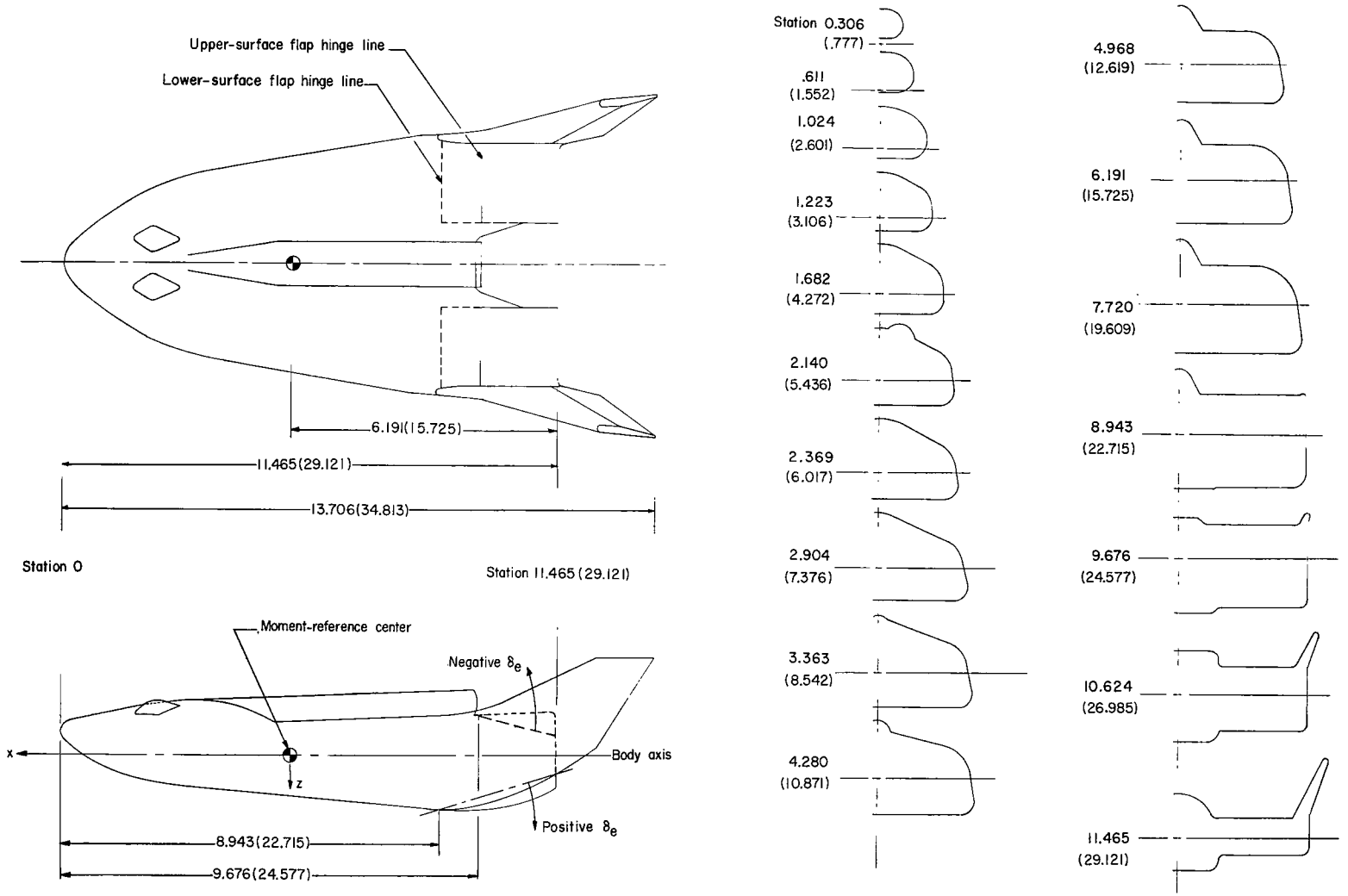

(c) Second stage.

Figure 1.- Concluded.

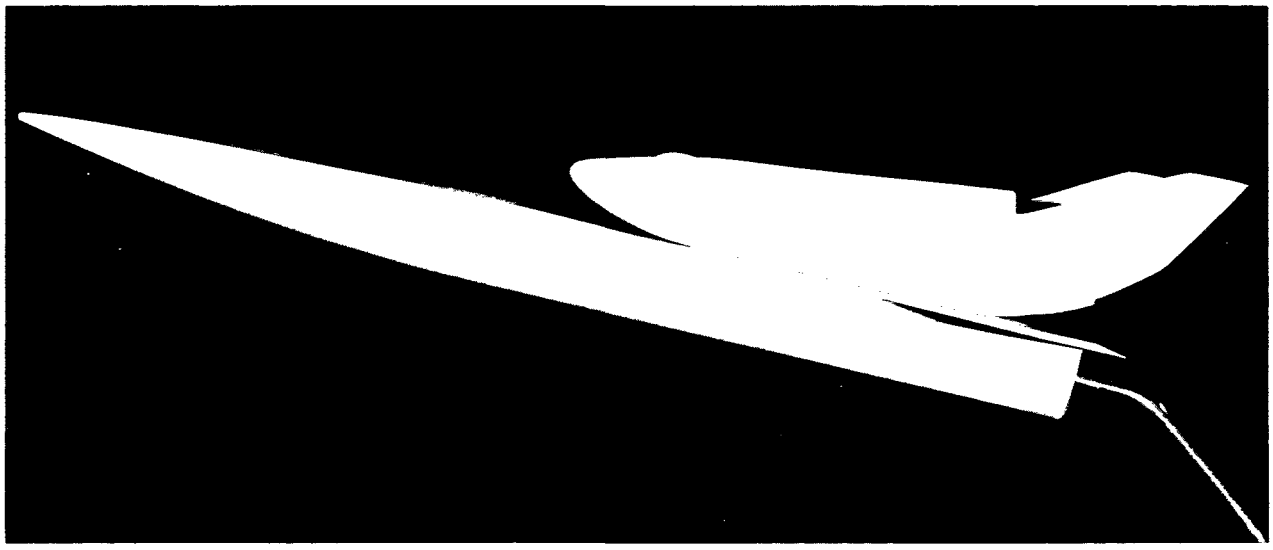

(a) Prior to stage separation. L-67-2939

(b) During stage separation maneuver.

Figure 2.- Photographs of launch vehicle system. L-67-2942

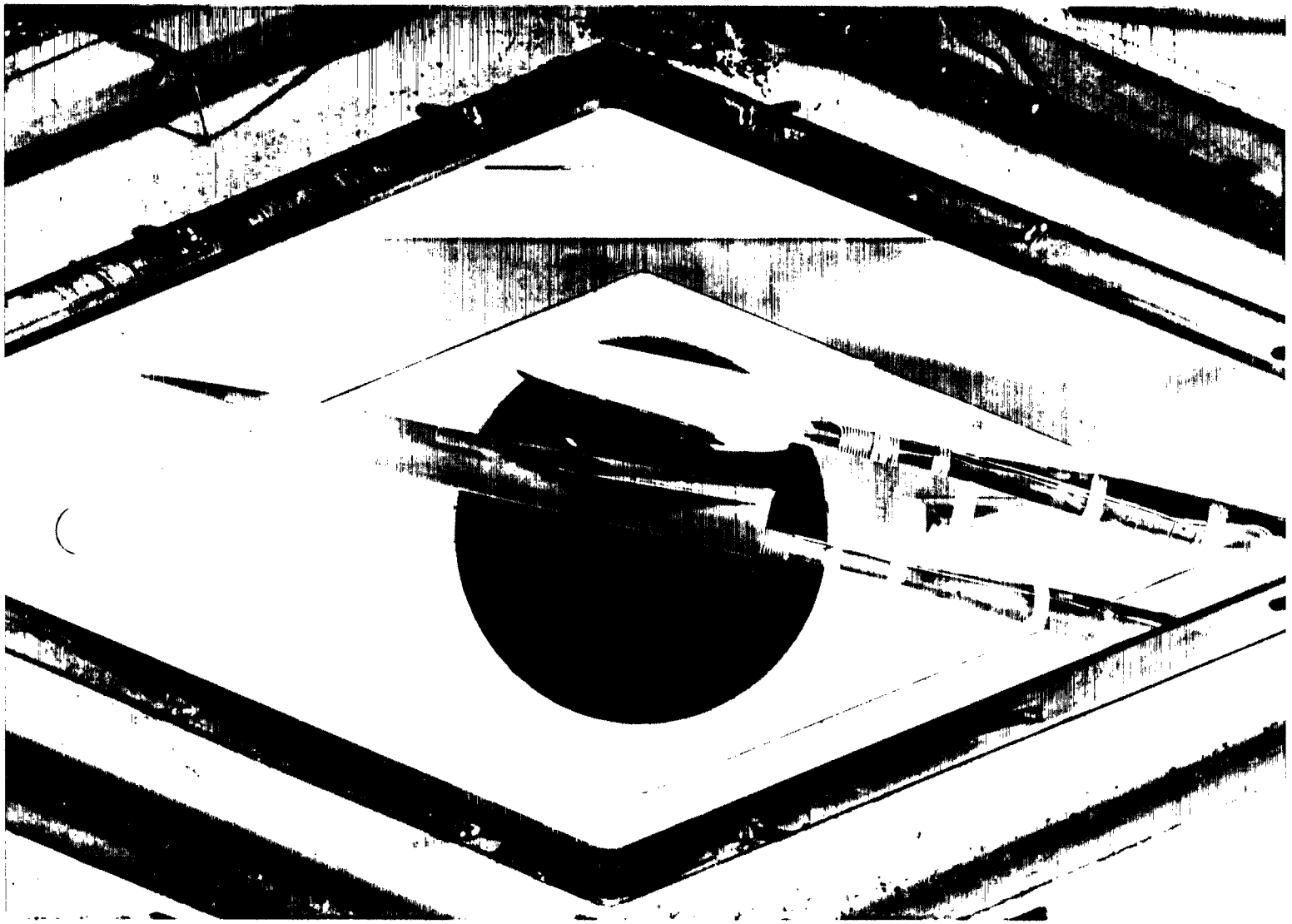

Figure 3.- Photograph of support apparatus.

L-67-3064

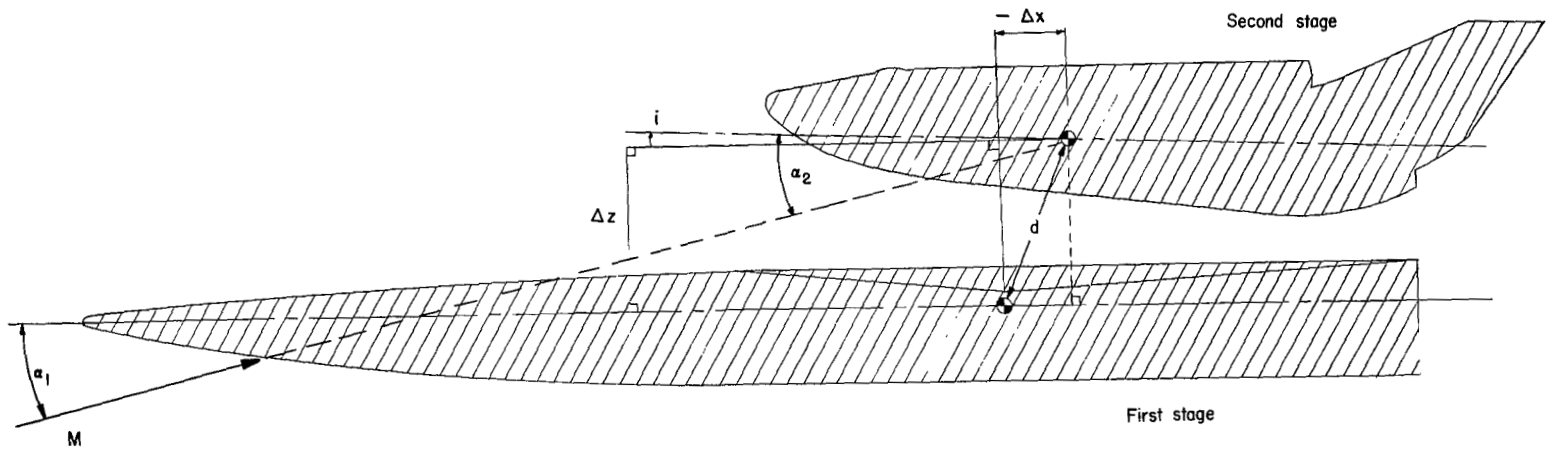

Figure 4.- Staging variables.

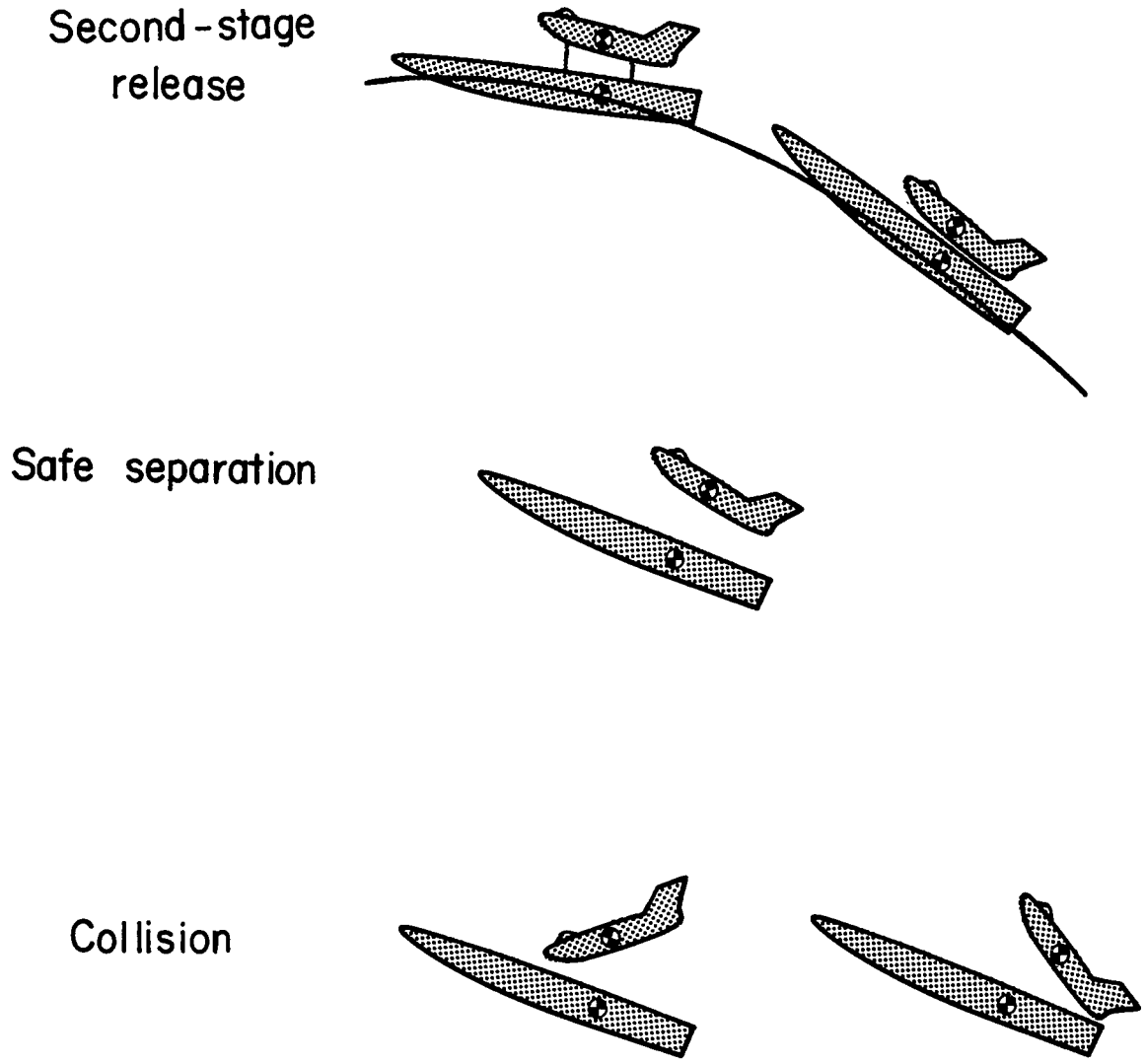

Figure 5.- Staging sequence.

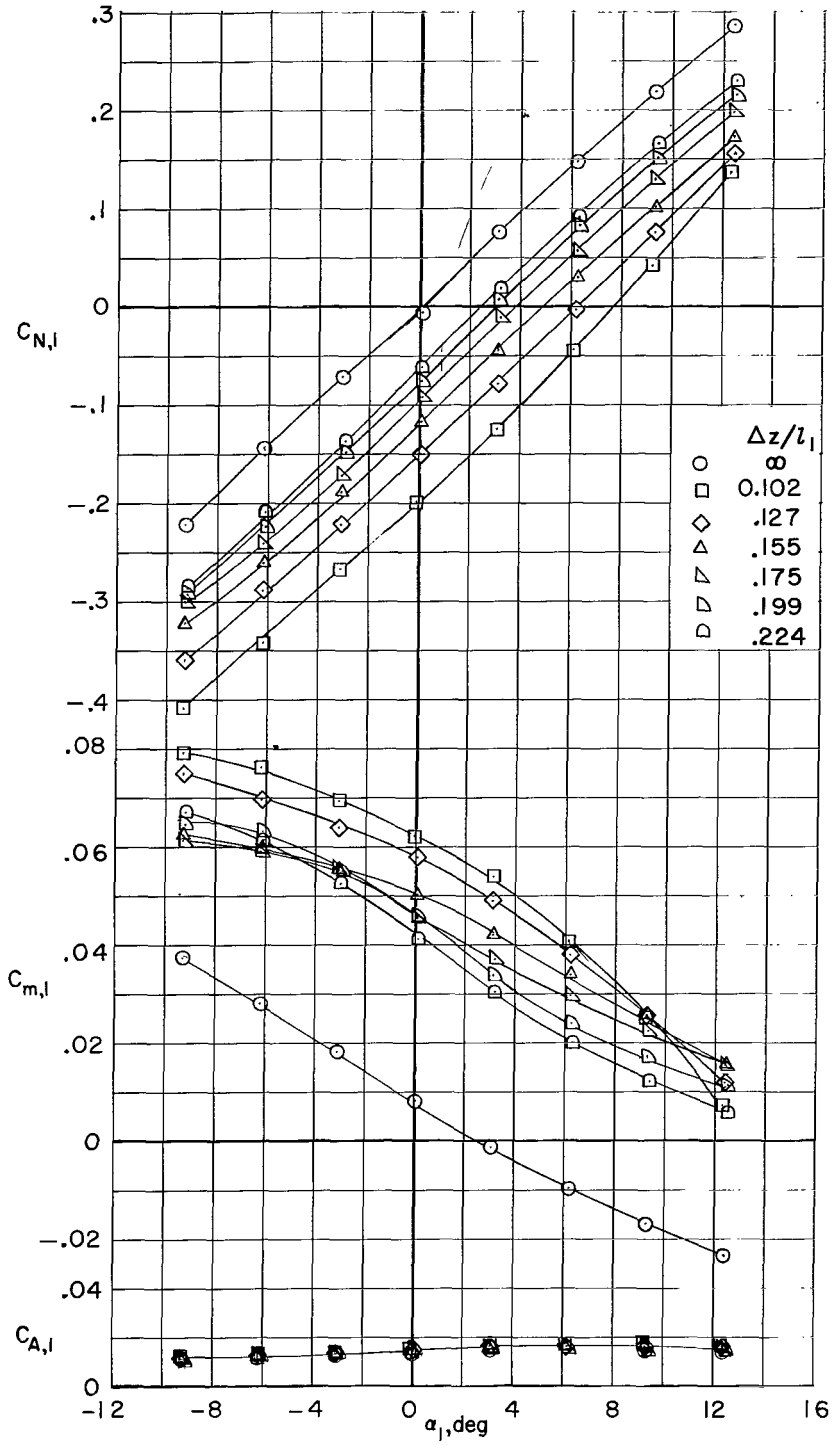

(a) $i = 0^0$; $\Delta x/l_1 = -0.051$.

Figure 6.- Longitudinal aerodynamic characteristics of the first stage at a Mach number of 3.

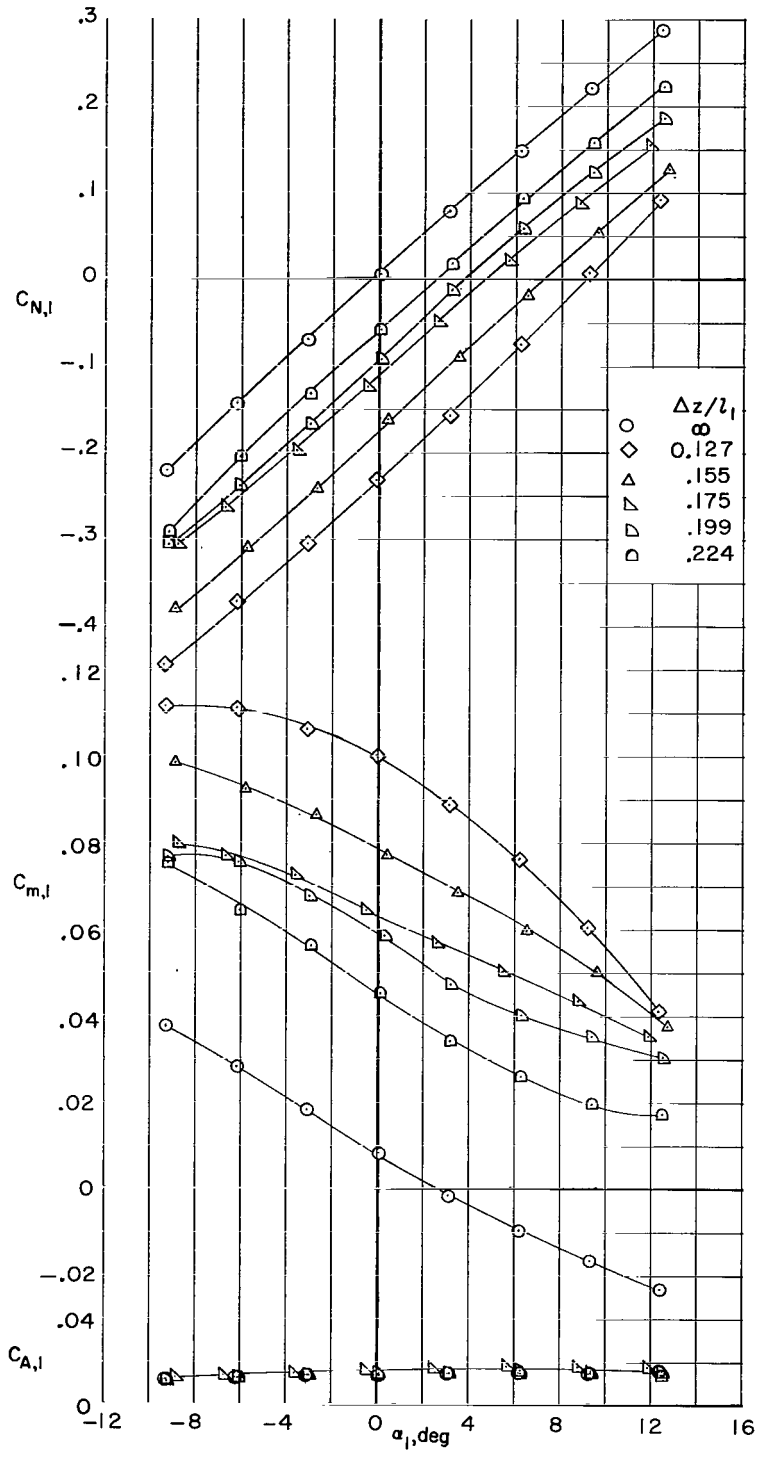

(b) $i = 5^0$; $\Delta x/l_1 = -0.051$.

Figure 6.- Continued.

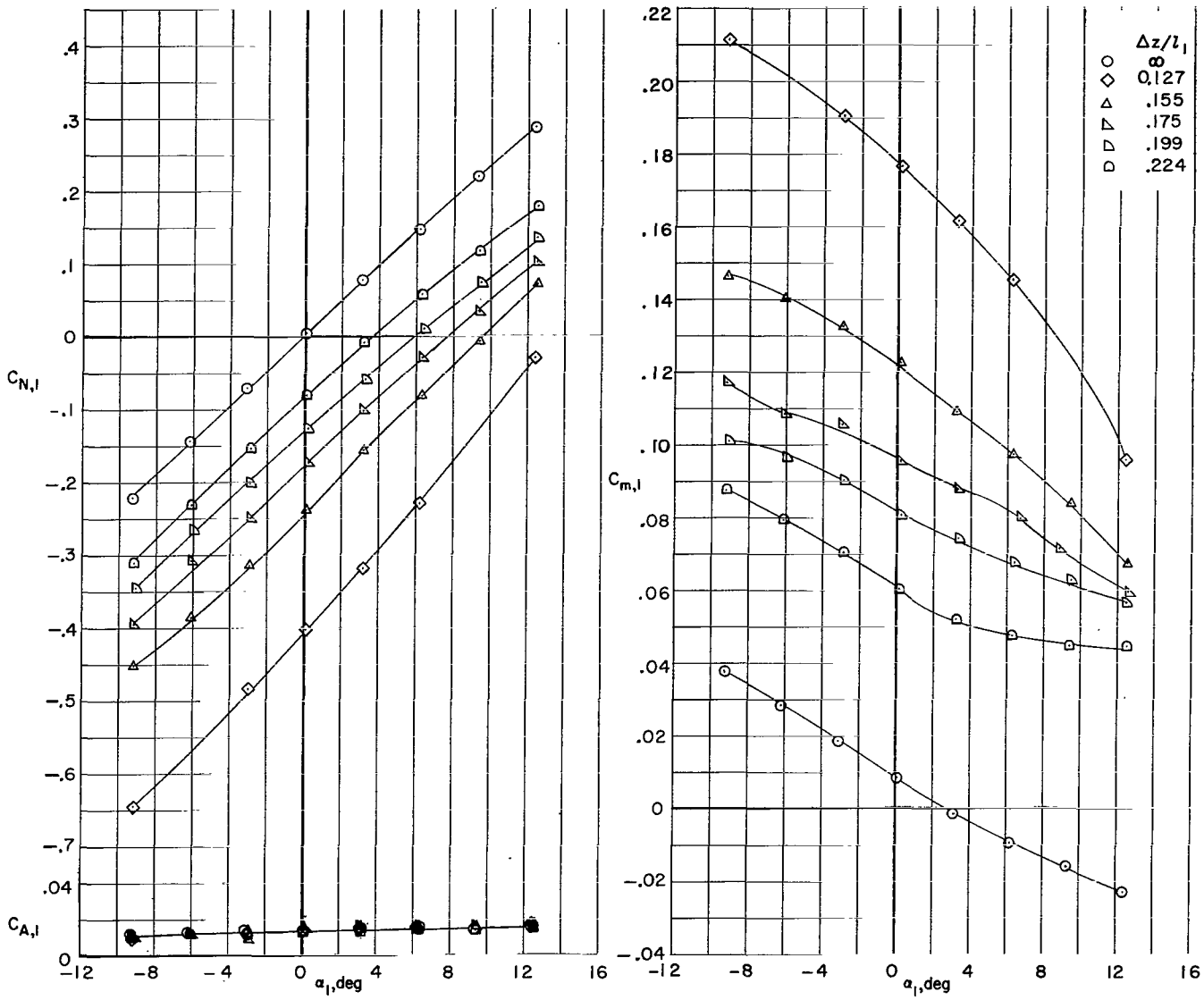

(c) $i = 10^0$; $\Delta x/l_1 = -0.051$.

Figure 6.- Continued.

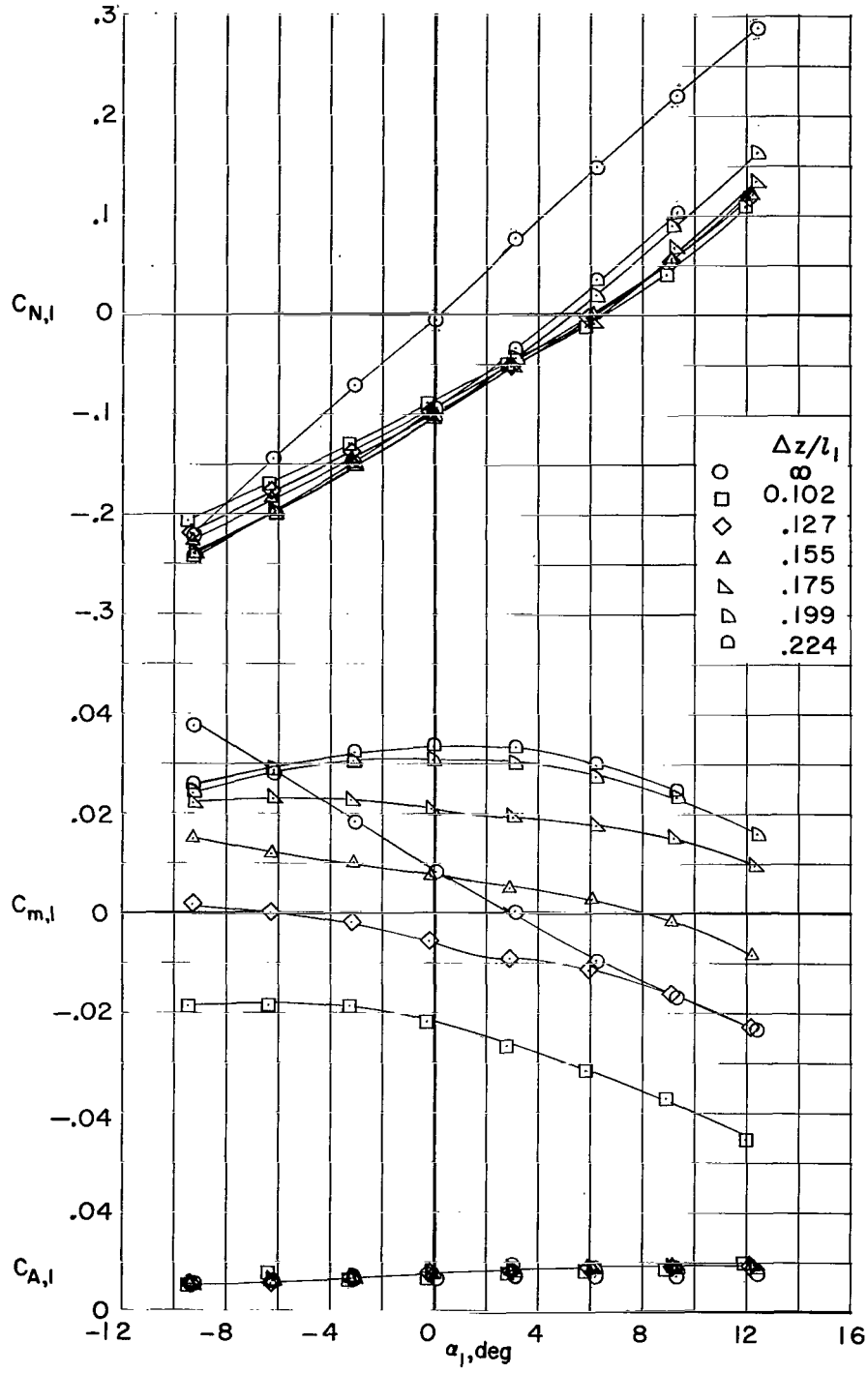

(d) $i = 0^0$; $\Delta x/l_l = 0.160$.

Figure 6.- Continued.

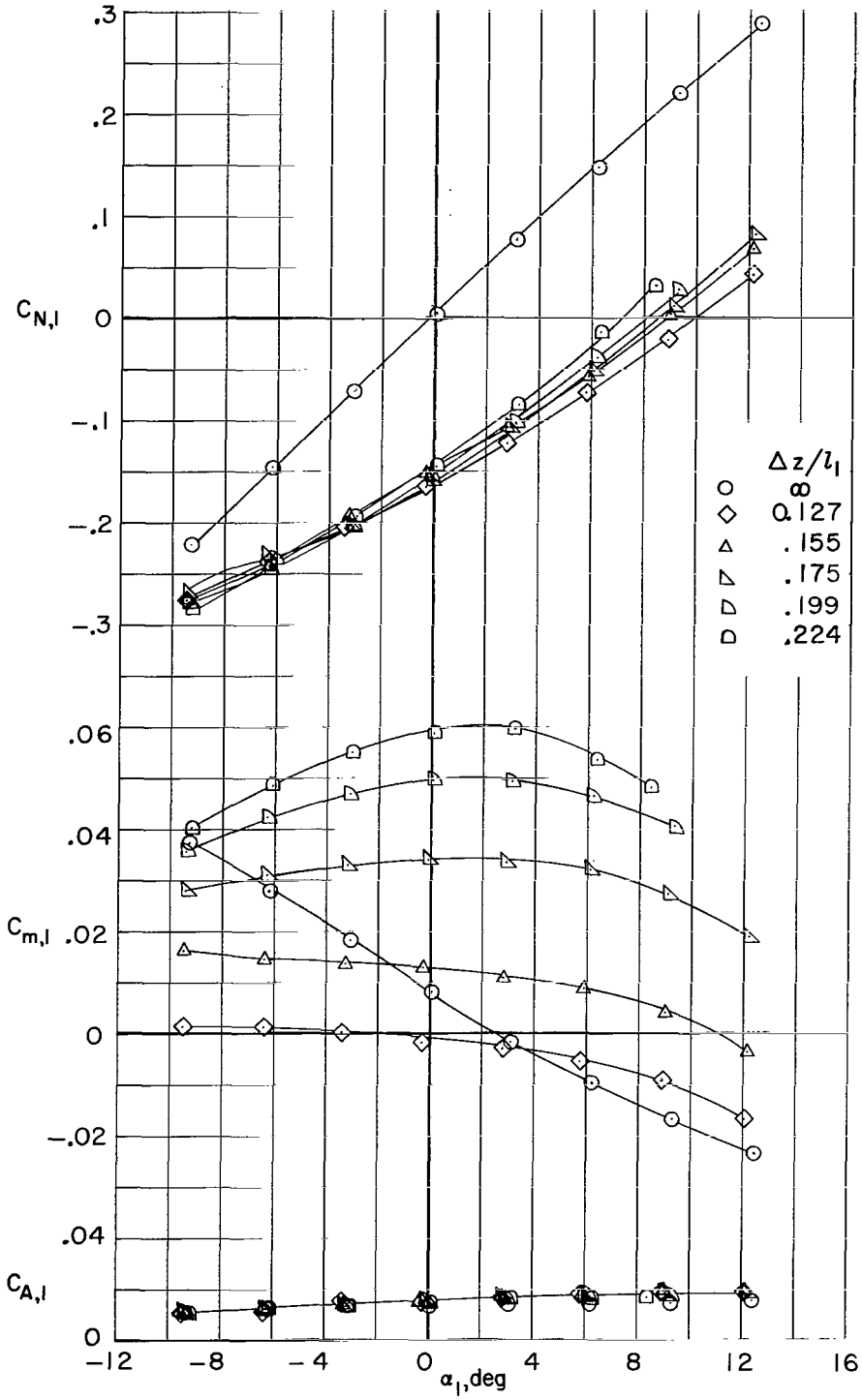

(e) $i = 5^0$; $\Delta x/l_l = 0.160$.

Figure 6.- Continued.

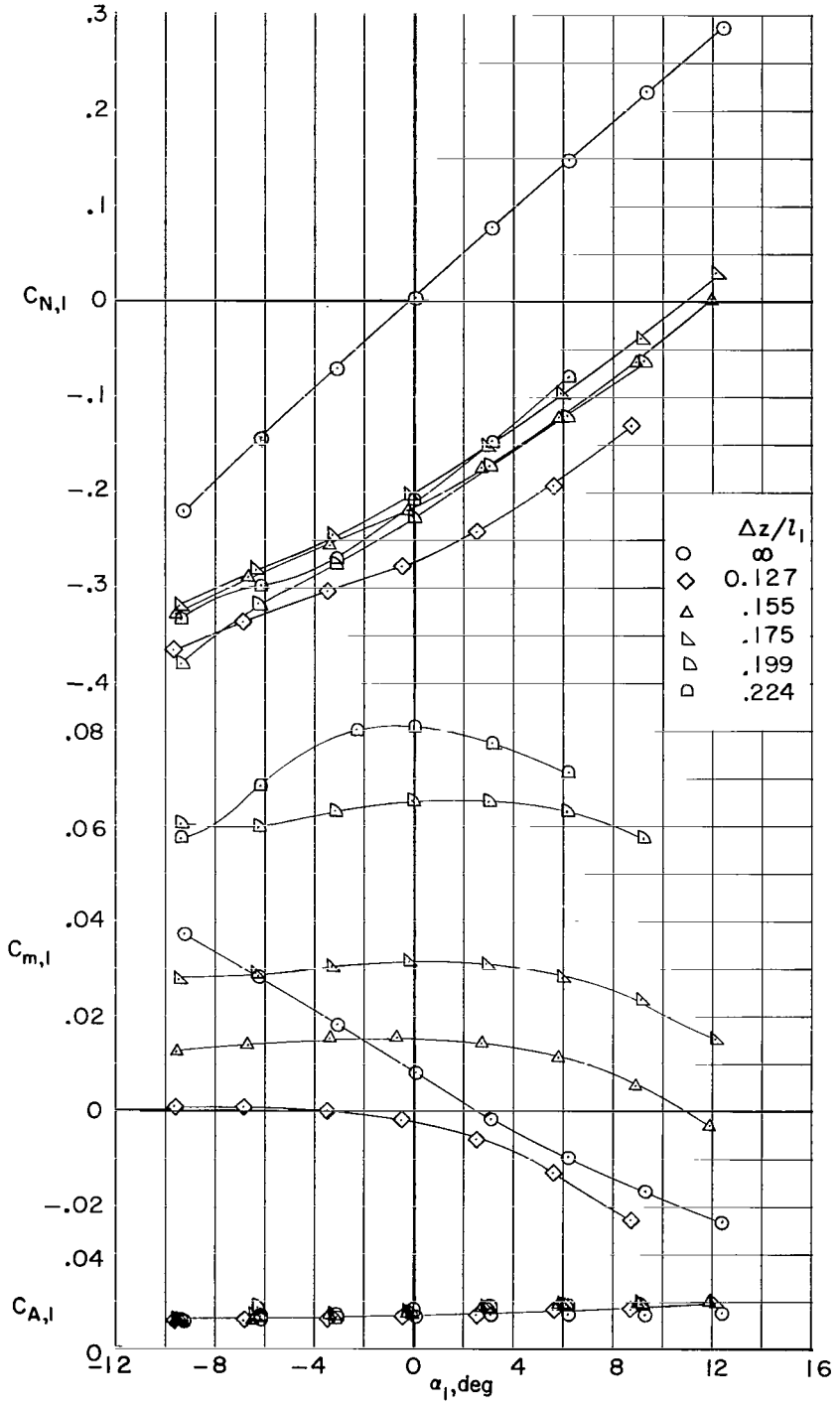

(f) i = 10°; $\Delta x/l_l$ = 0.160.

Figure 6.- Concluded.

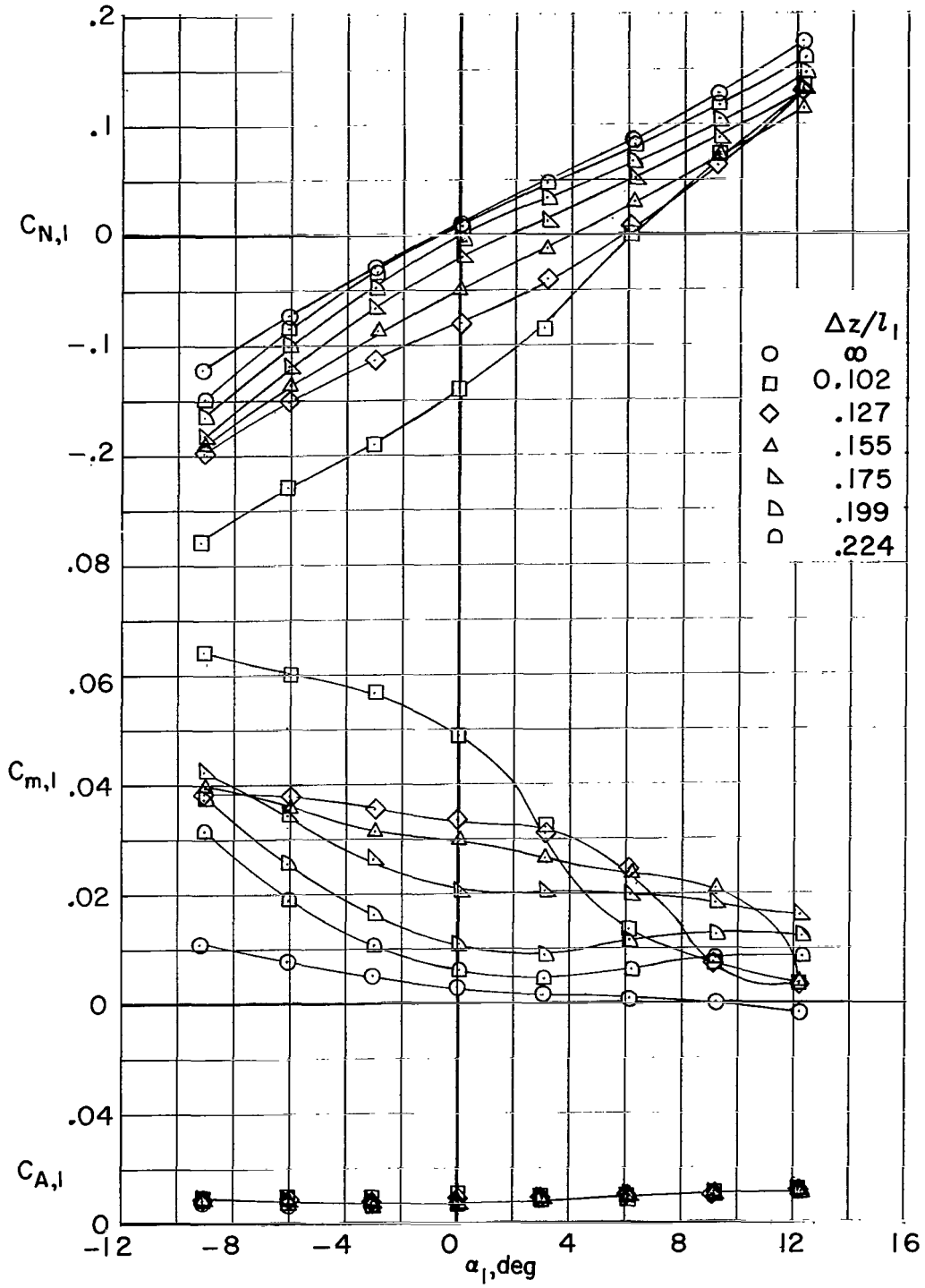

(a) $i = 0^0$; $\Delta x/l_1 = -0.051$.

Figure 7.- Longitudinal aerodynamic characteristics of the first stage at a Mach number of 6.

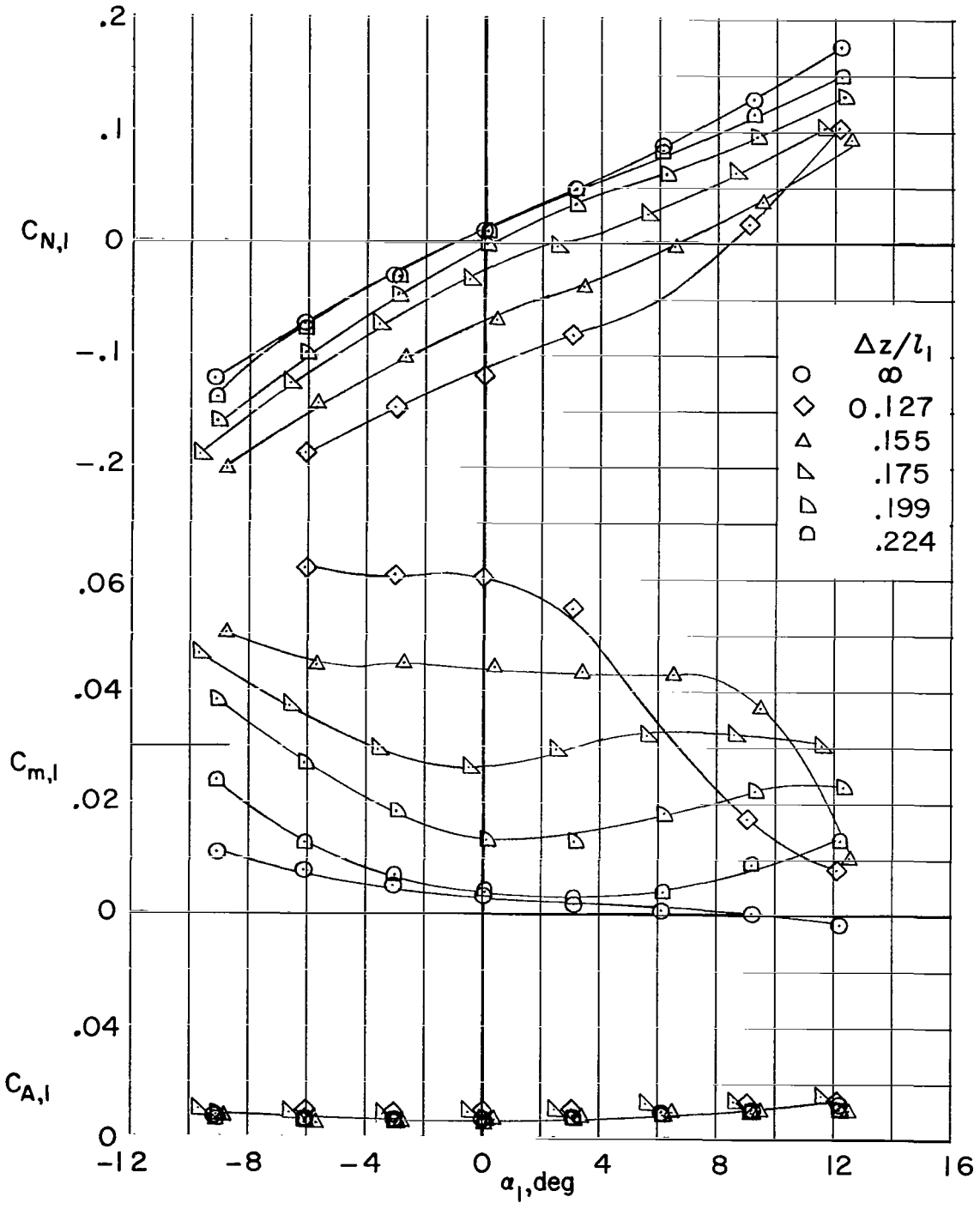

(b) i = 5°; $\Delta x/l_1$ = -0.051.

Figure 7.- Continued.

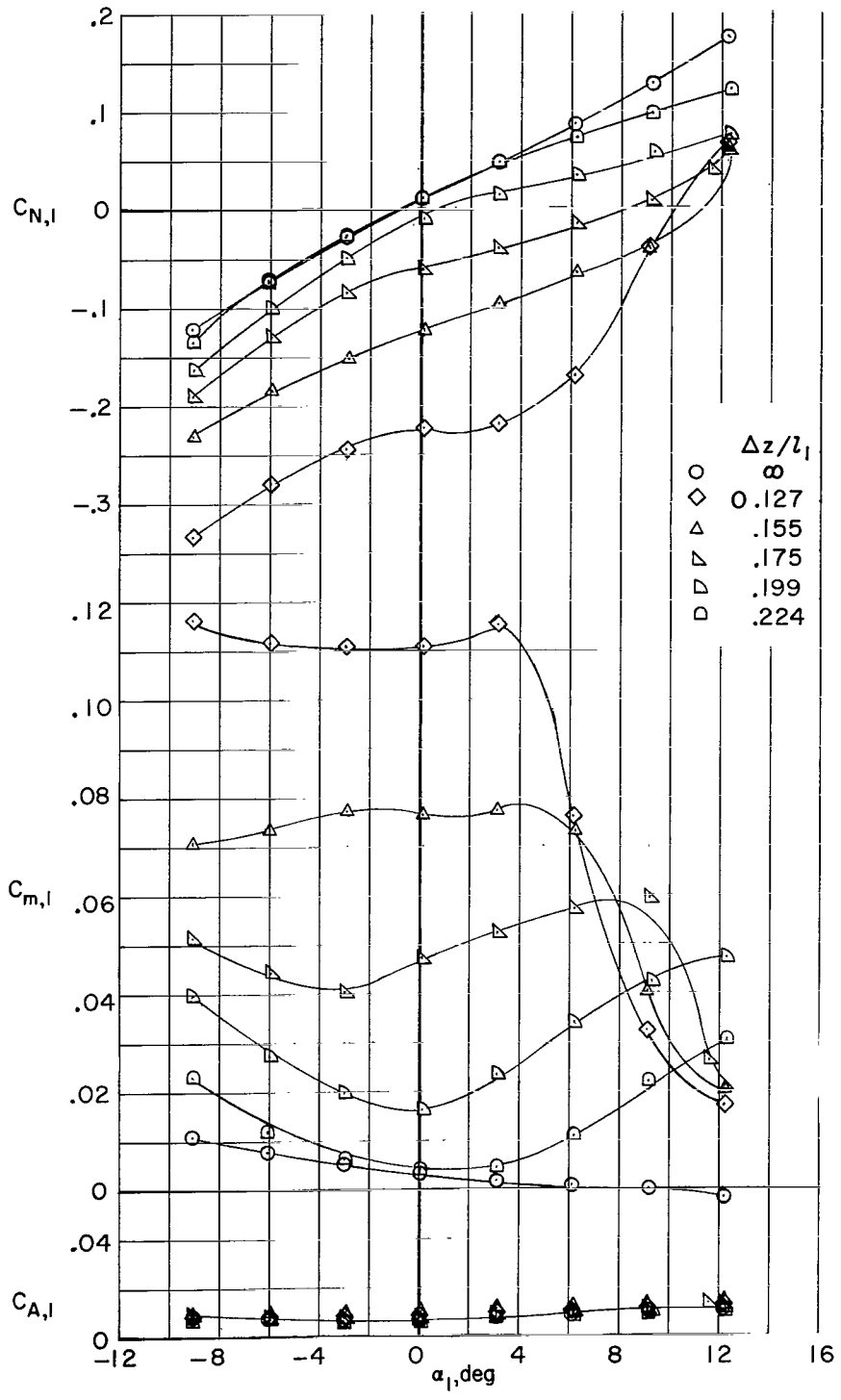

(c) i = 10°; $\Delta x/l_l$ = -0.051.

Figure 7.- Continued.

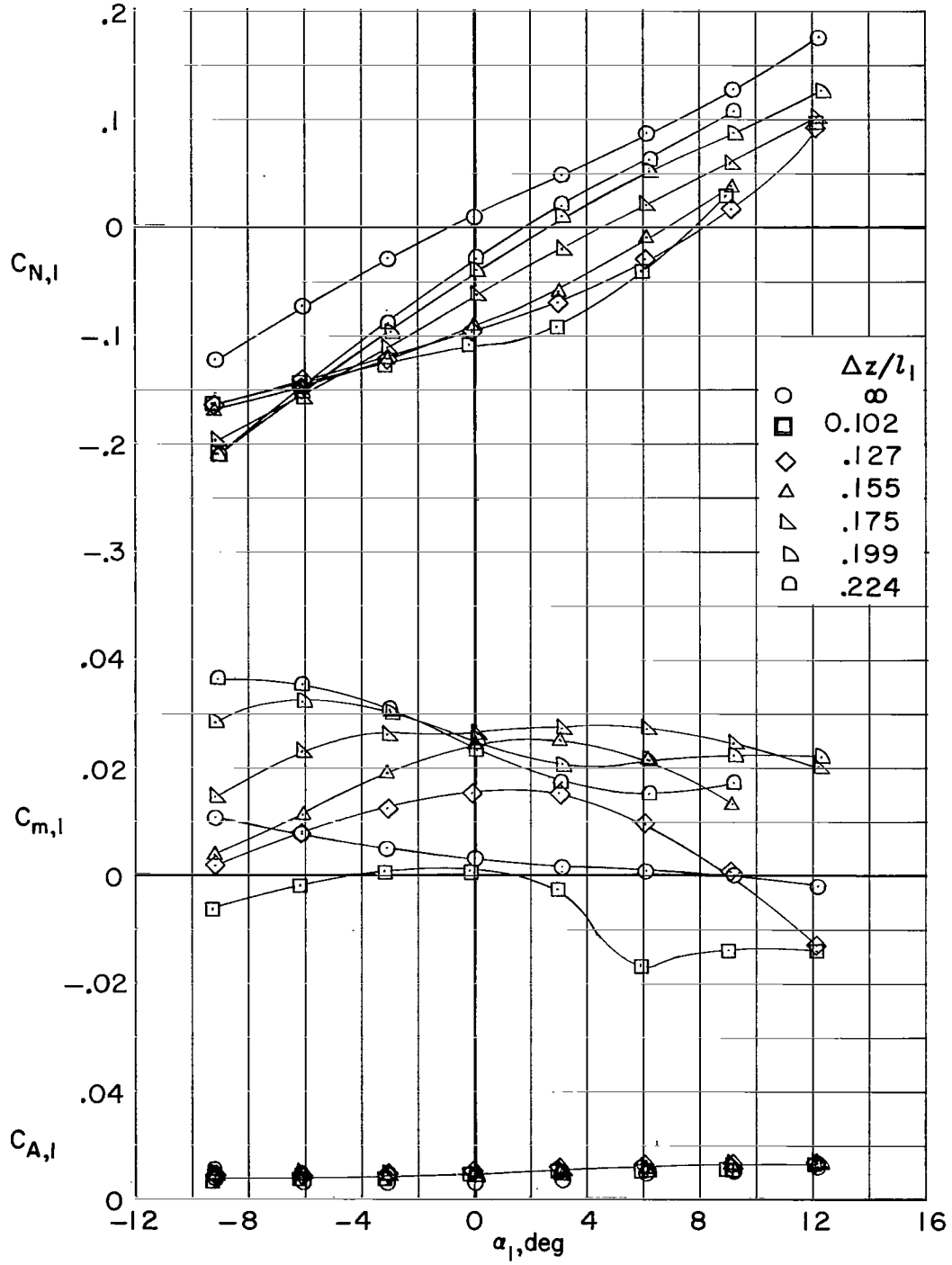

(d) $i = 0^{o}$; $\Delta x/l_1 = 0.160$.

Figure 7.- Continued.

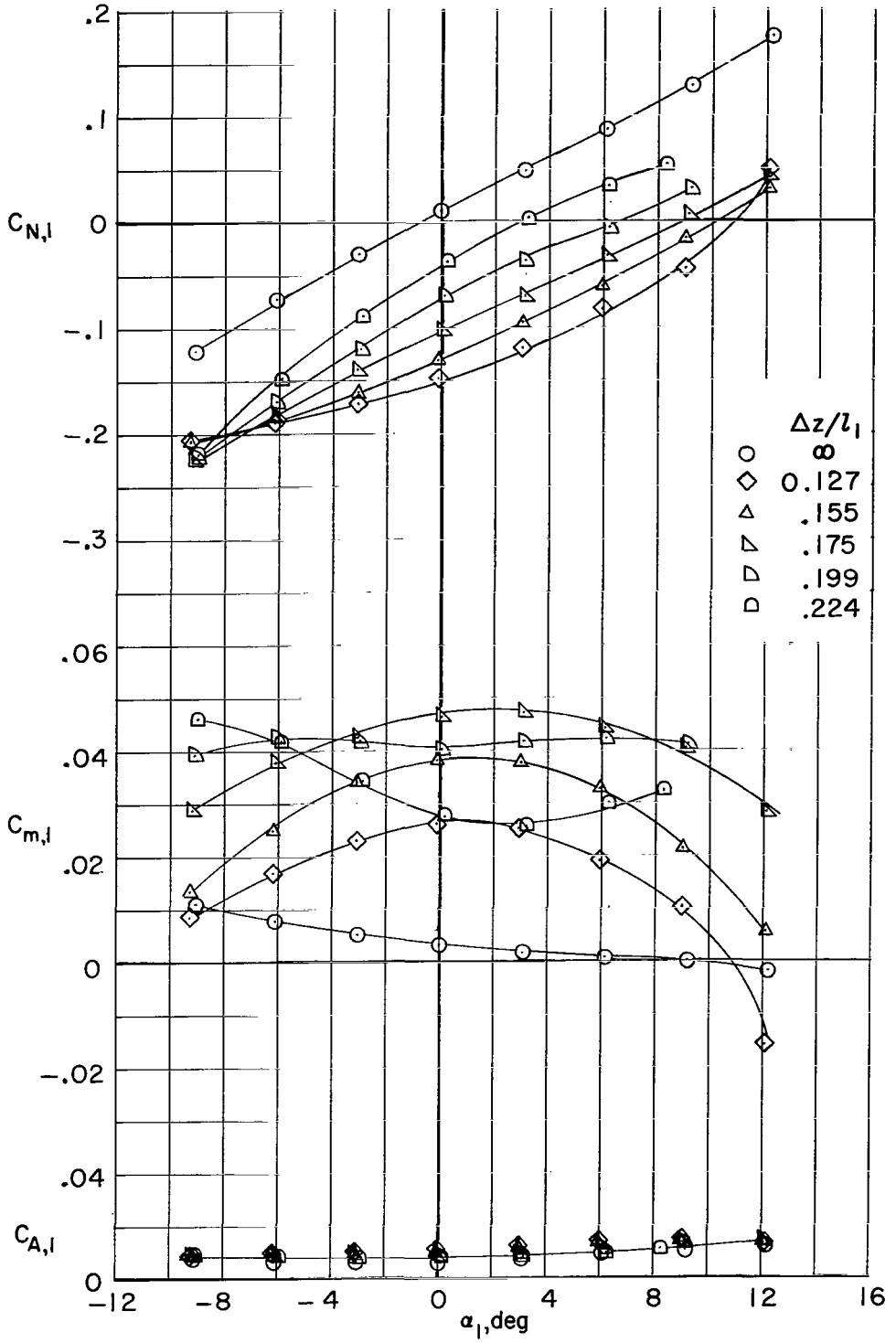

(e) i = 5°; $\Delta x/l_l = 0.160$.

Figure 7.- Continued.

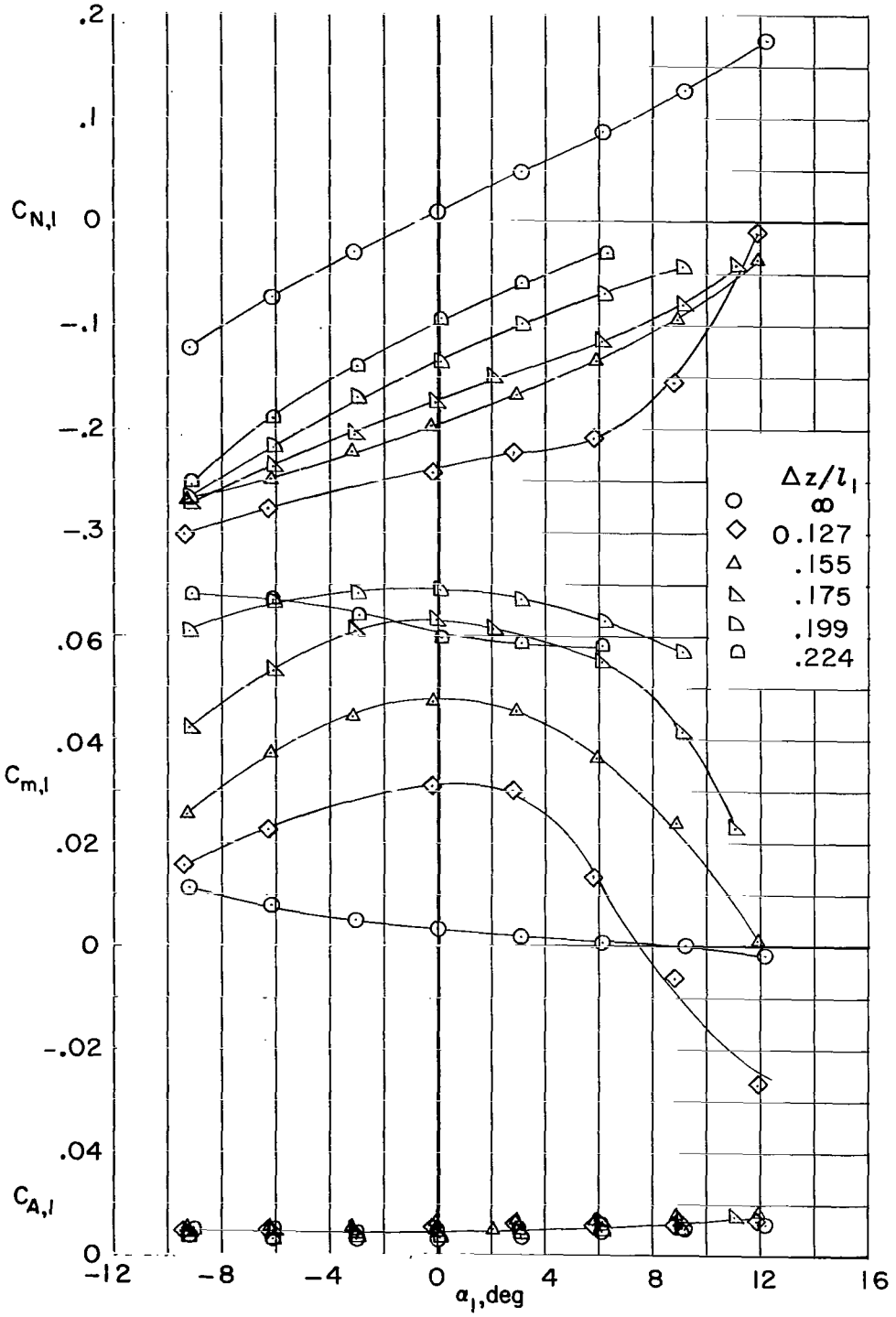

(f) i = 10°; $\Delta x/l_1 = 0.160$.

Figure 7.- Concluded.

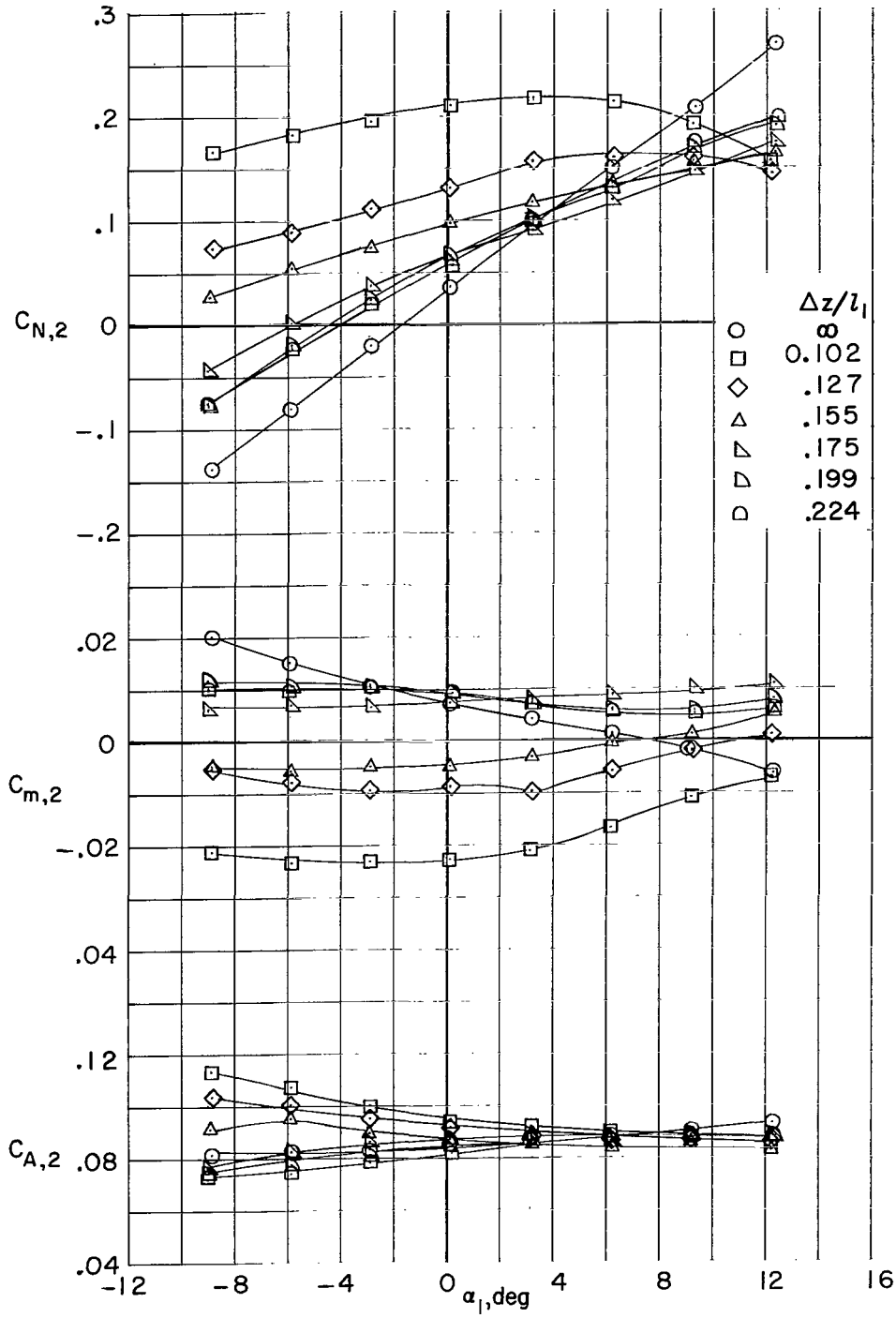

(a) $i = 0^0$; $\Delta x/l_1 = -0.051$.

Figure 8.- Longitudinal aerodynamic characteristics of the second stage at a Mach number of 3.

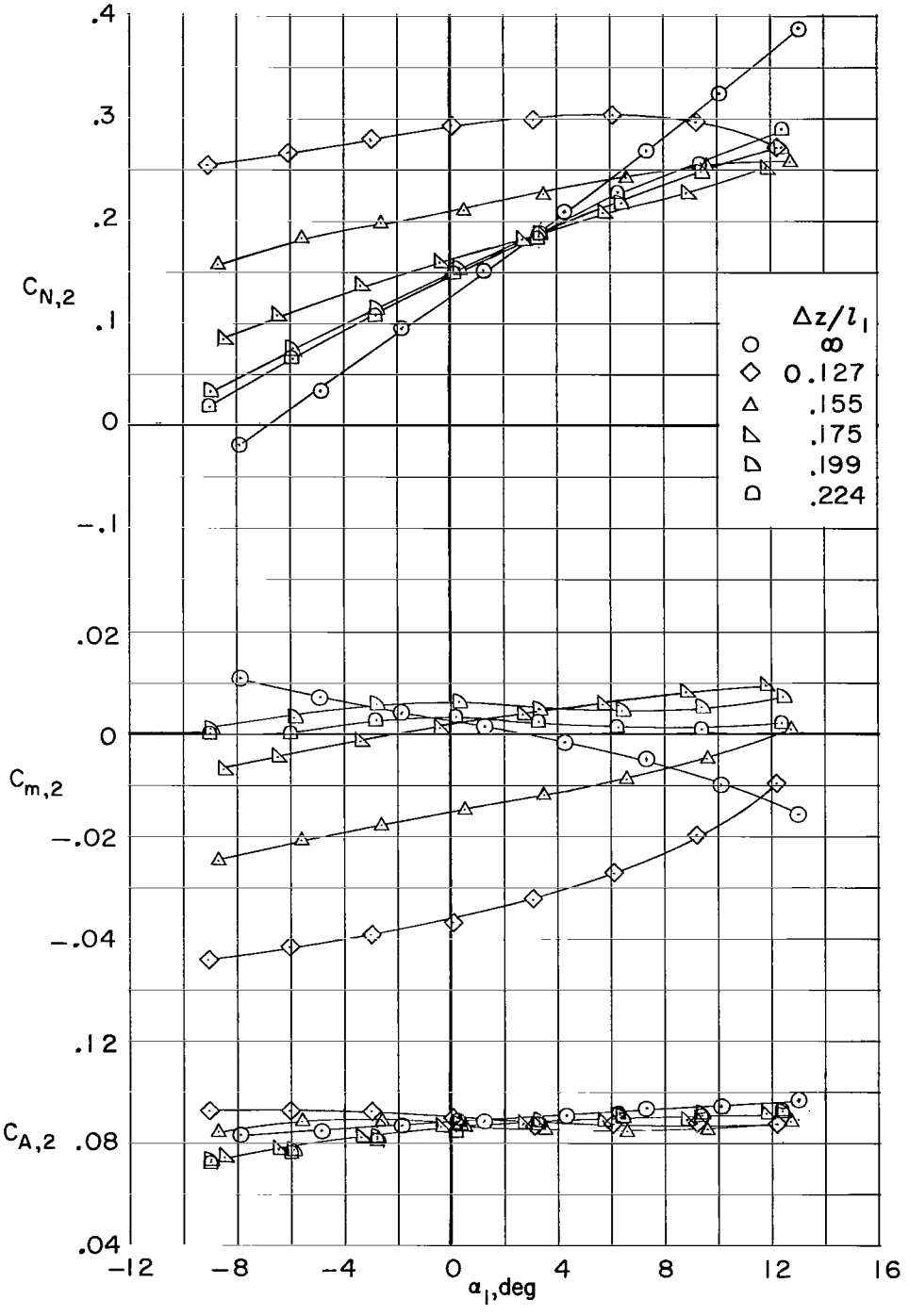

(b) $i = 5^0$; $\Delta x/l_1 = -0.051$.

Figure 8.- Continued.

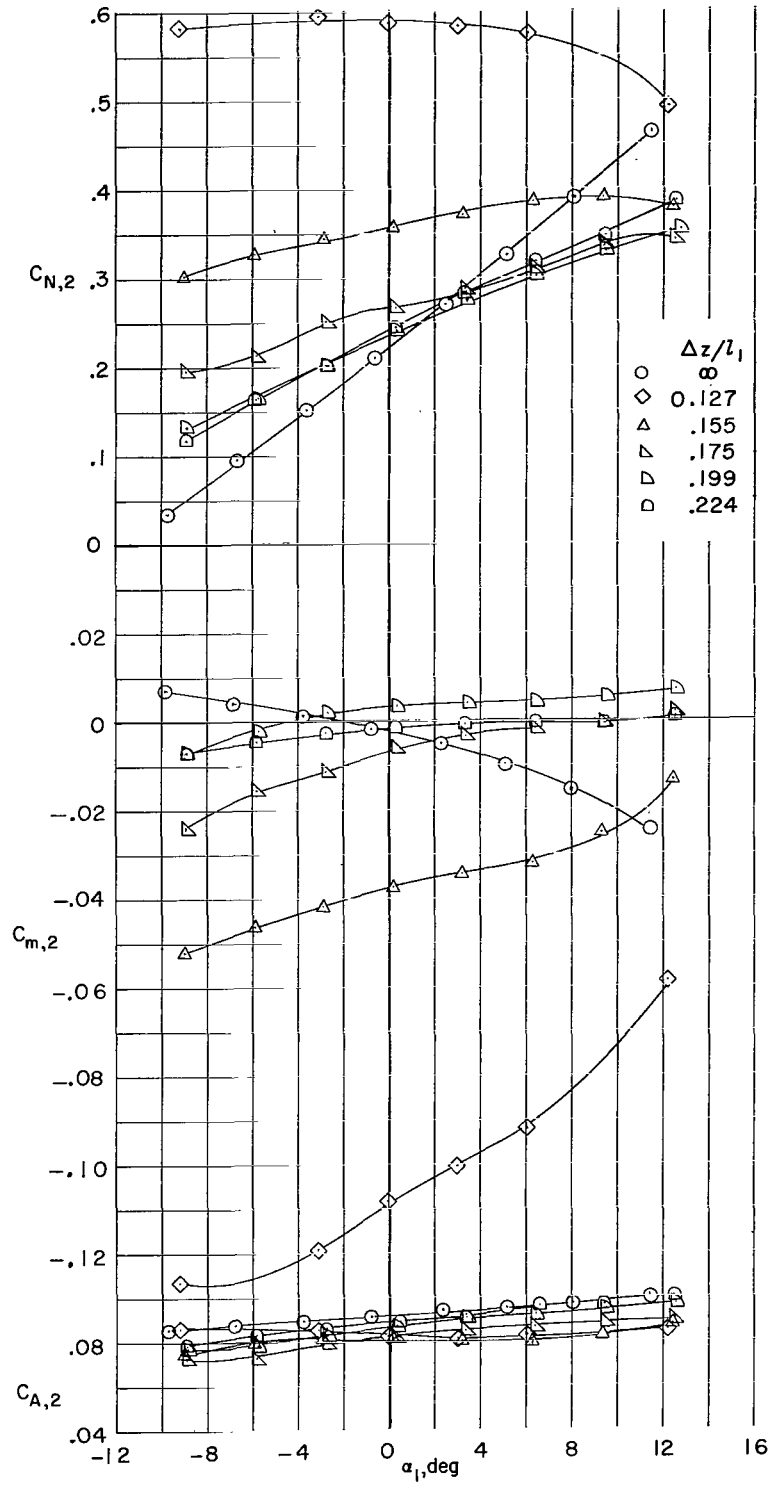

(c) i = 10°; $\Delta x/l_1$ = -0.051.

Figure 8.- Continued.

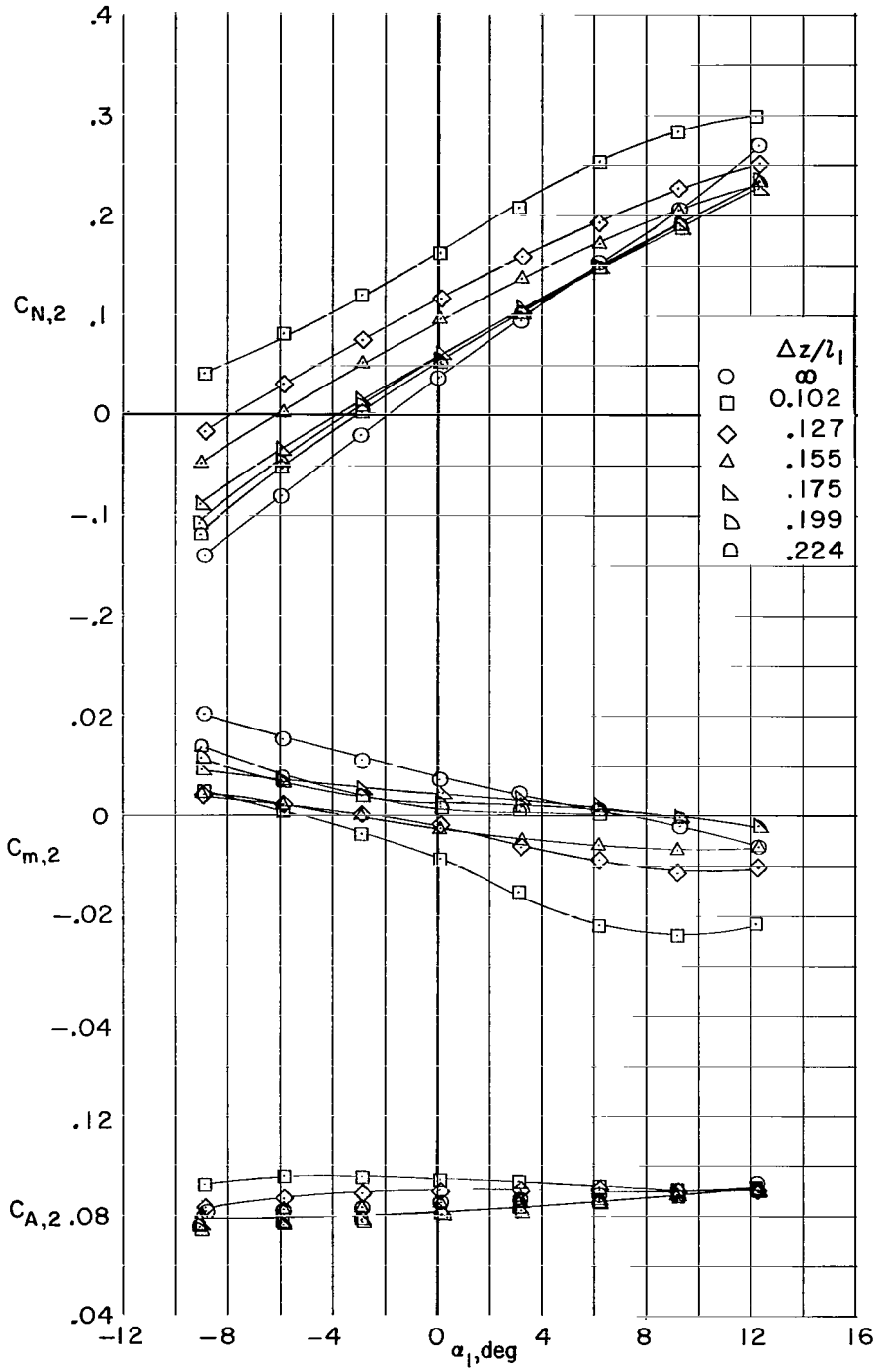

(d) $i = 0^0$; $\Delta x/l_1 = 0.160$.

Figure 8.- Continued.

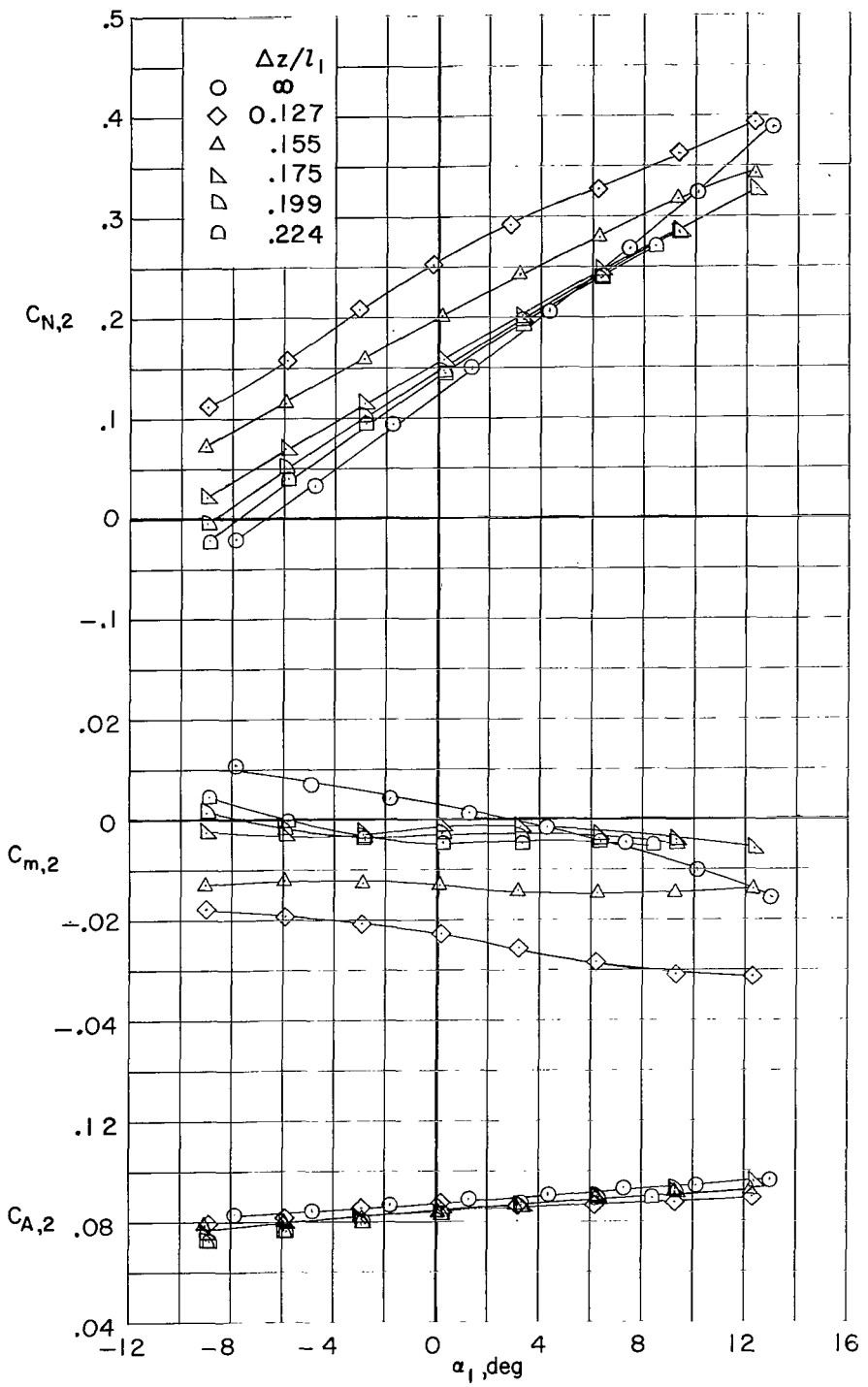

(e) $i = 5^0$; $\Delta x/l_1 = 0.160$.

Figure 8.- Continued.

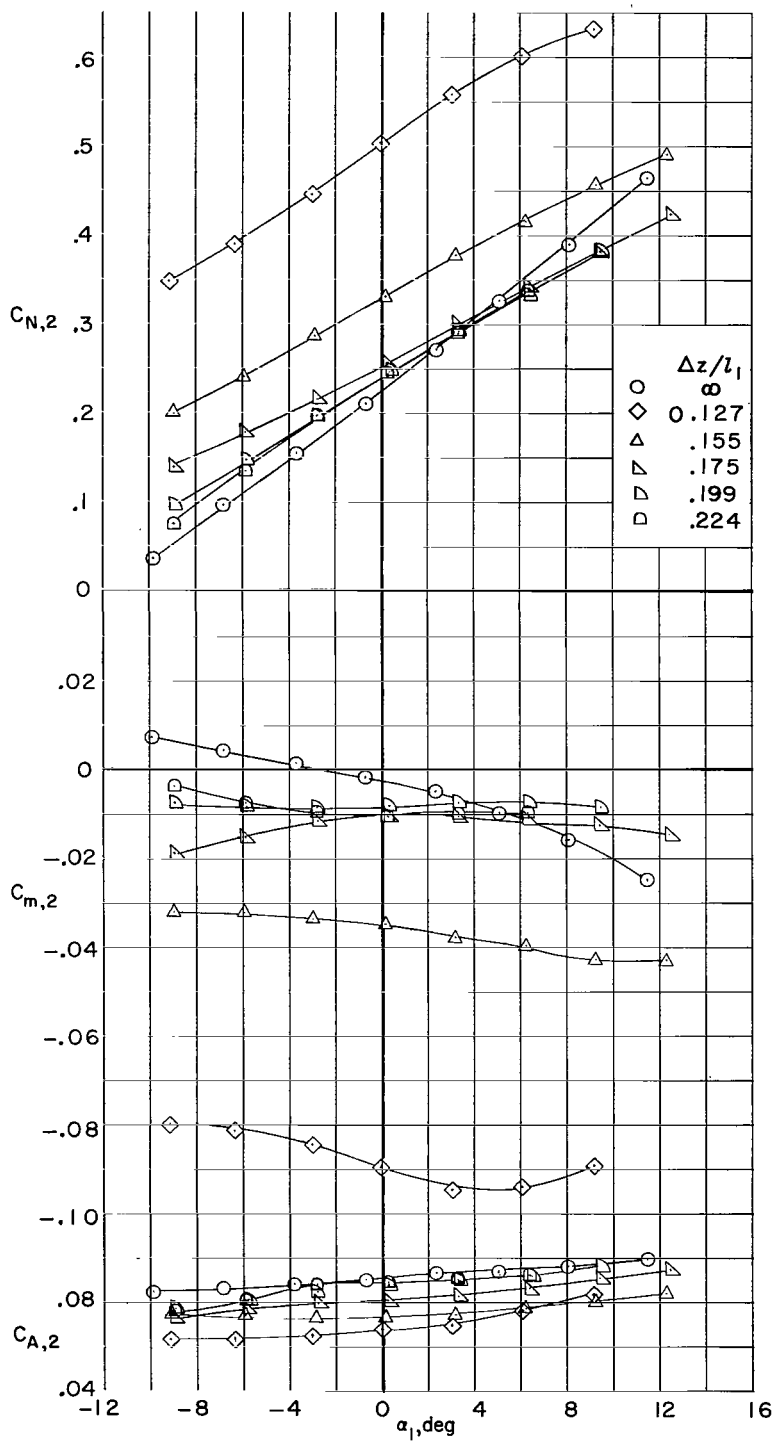

(f) $i = 10^0$; $\Delta x/l_1 = 0.160$.

Figure 8.- Concluded.

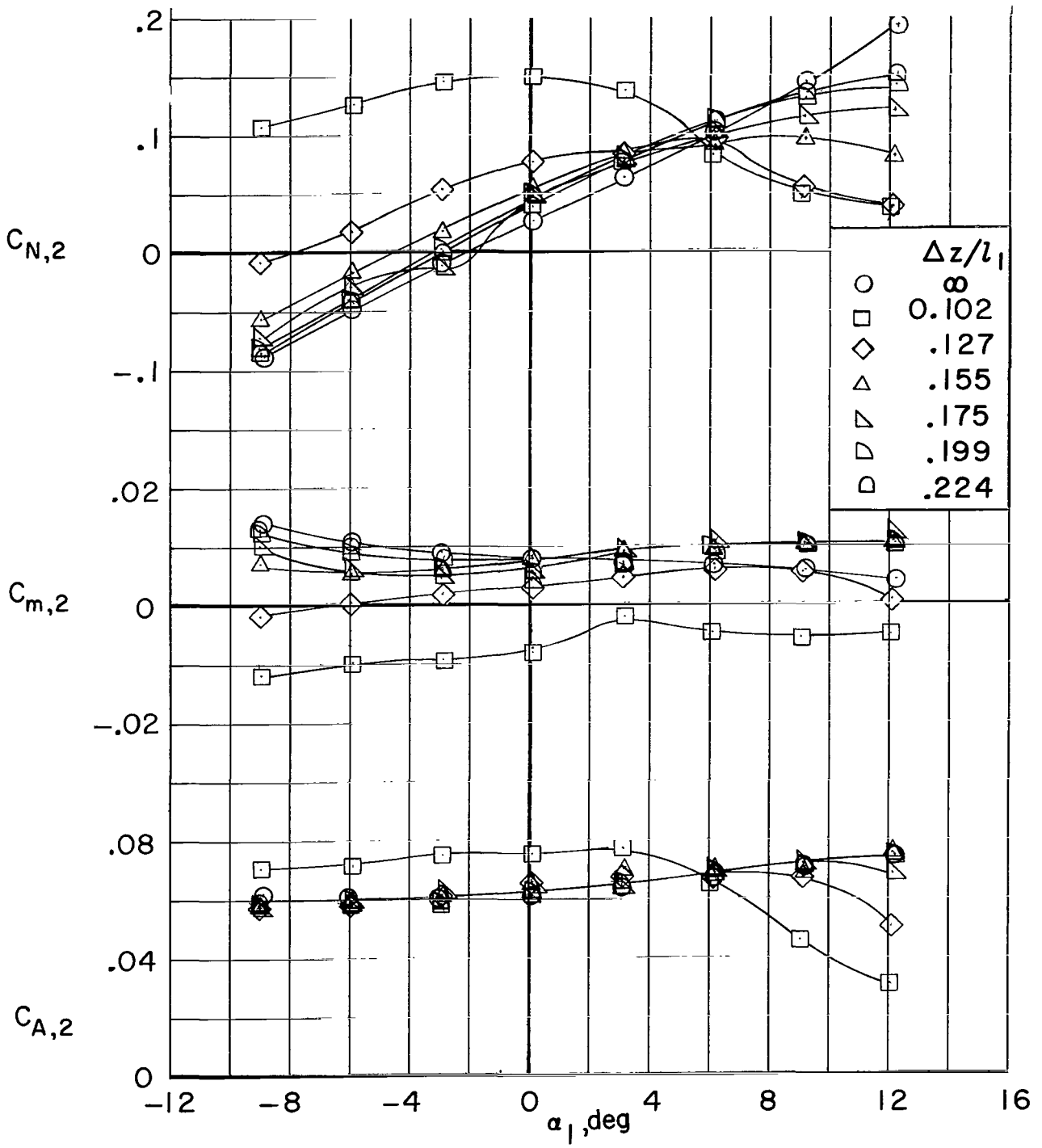

(a) $i = 0^0$; $\Delta x/l_1 = -0.051$.

Figure 9.- Longitudinal aerodynamic characteristics of the second stage at a Mach number of 6.

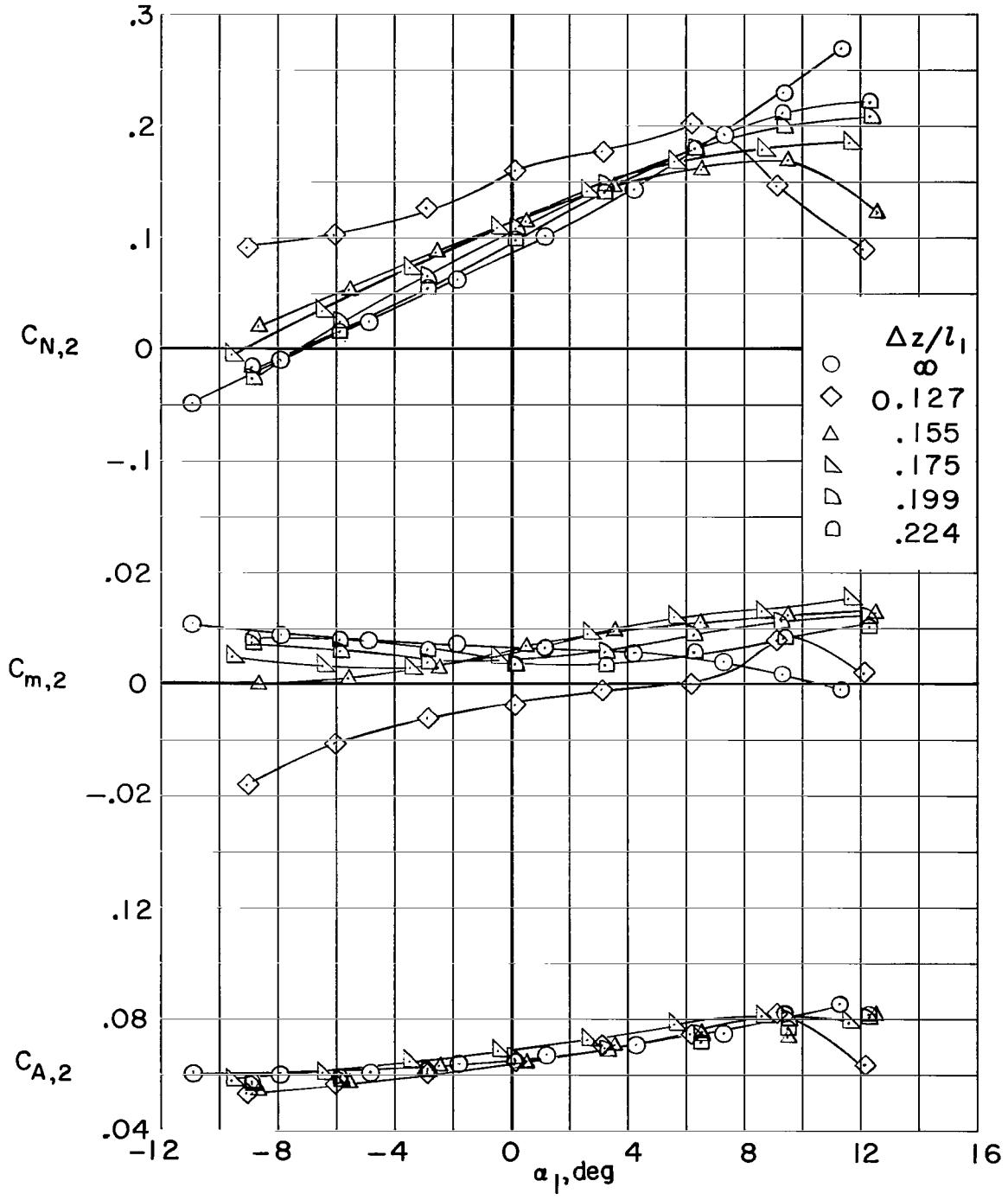

(b) $i = 5^0$; $\Delta x/l_1 = -0.051$.

Figure 9.- Continued.

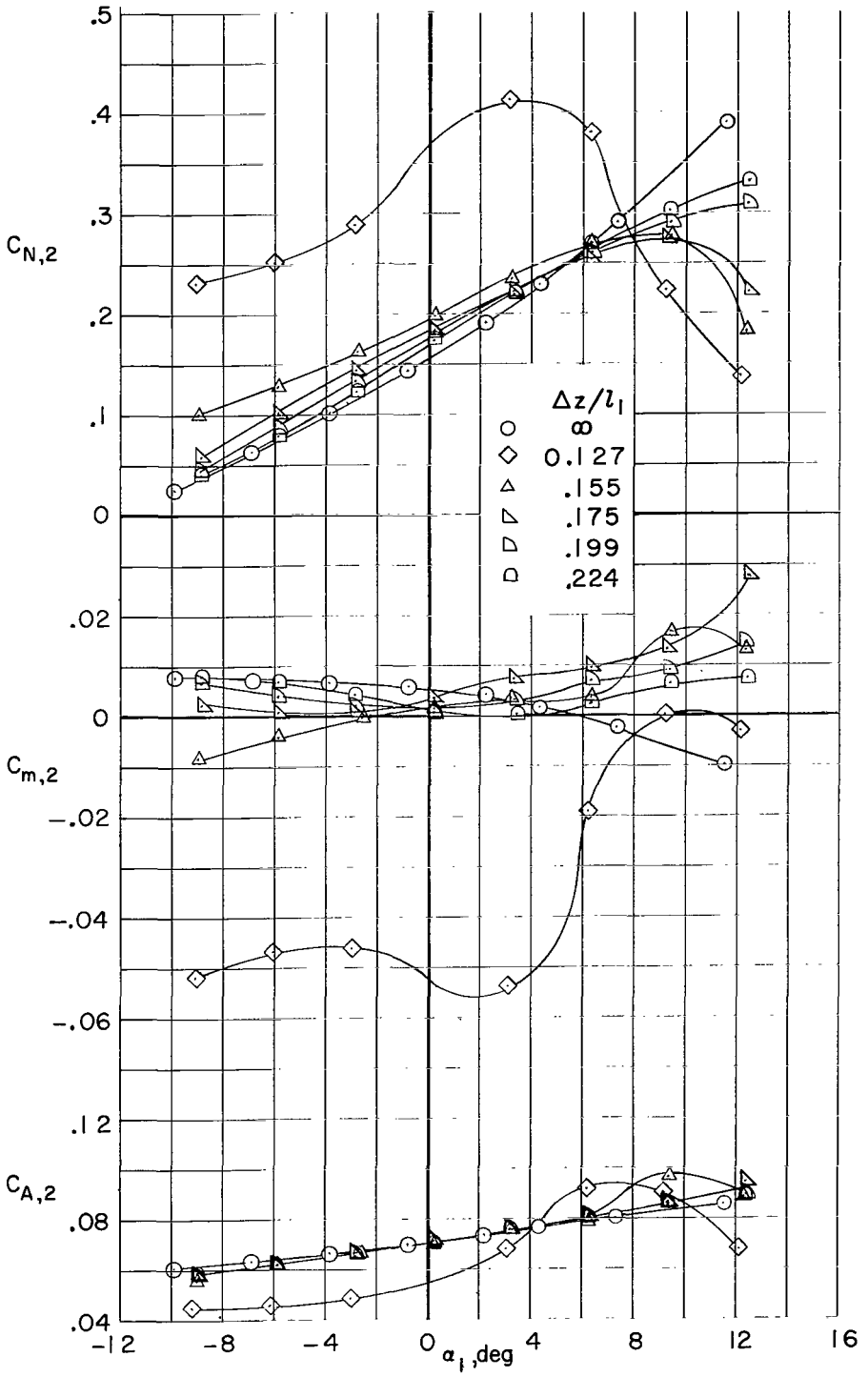

(c) $i = 10^0$; $\Delta x/l_1 = -0.051$.

Figure 9.- Continued.

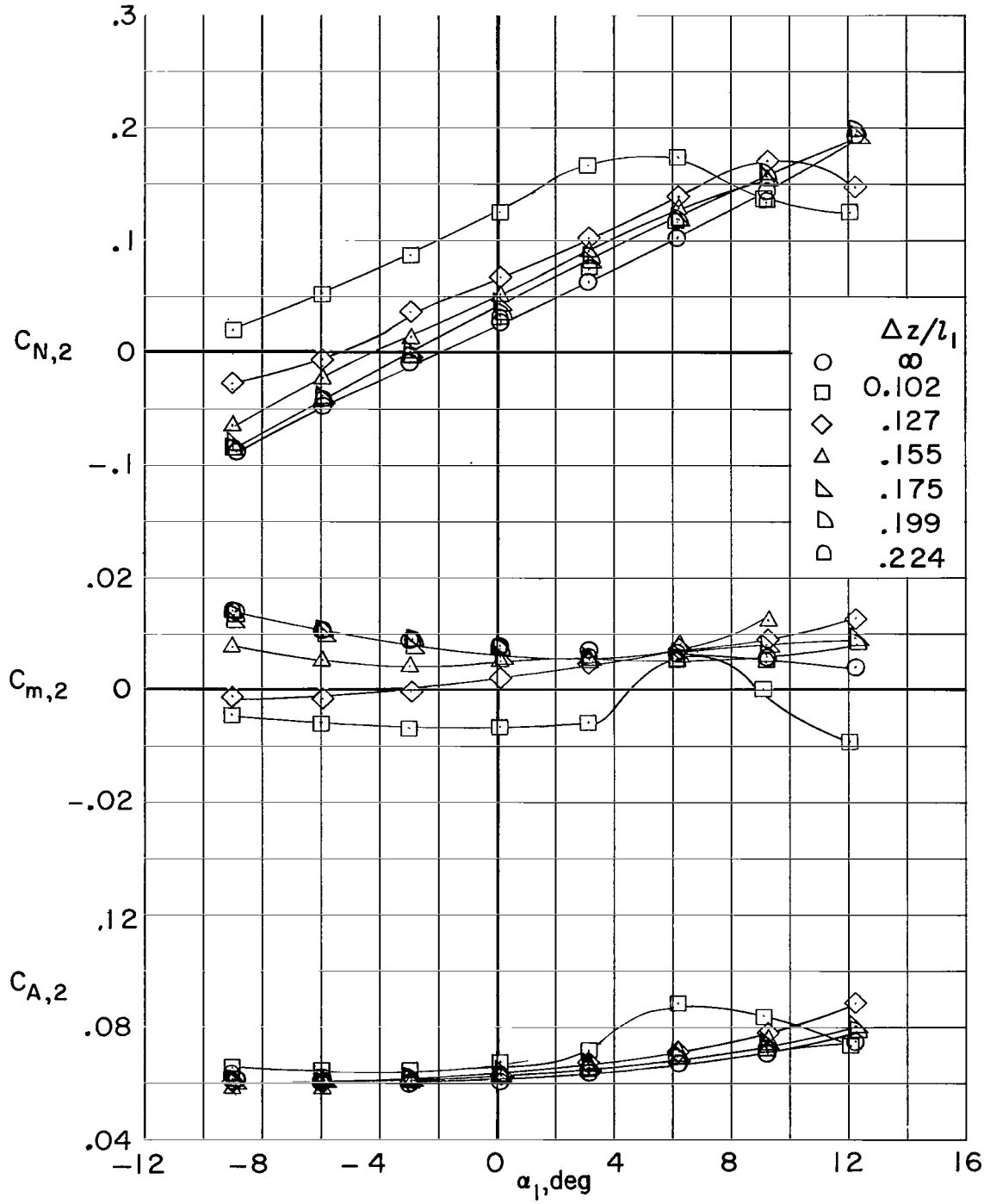

(d) $i = 0^0$; $\Delta x/l_1 = 0.160$.

Figure 9.- Continued.

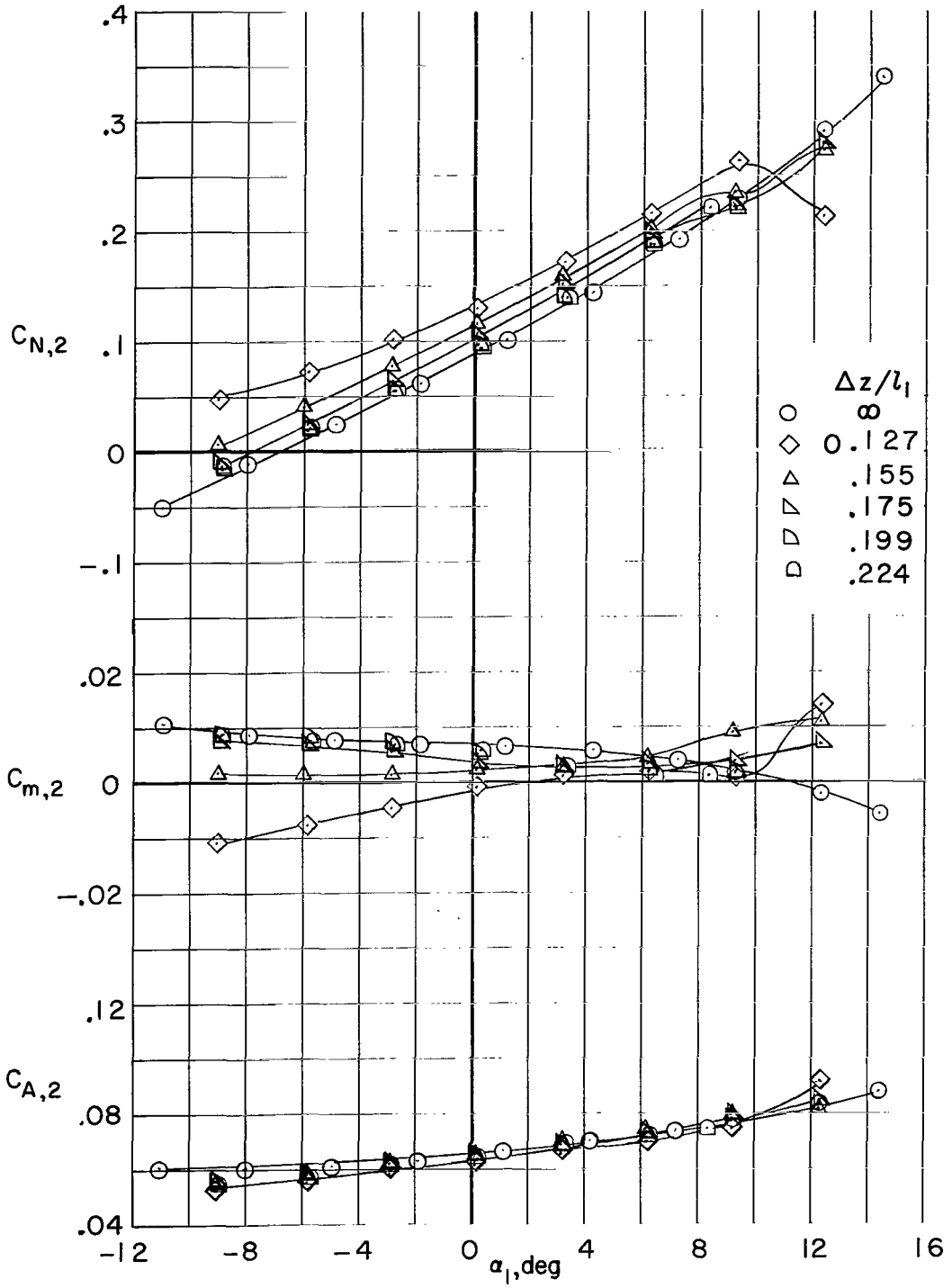

(e) $i = 5^0$; $\Delta x/l_1 \approx 0.160$.

Figure 9.- Continued.

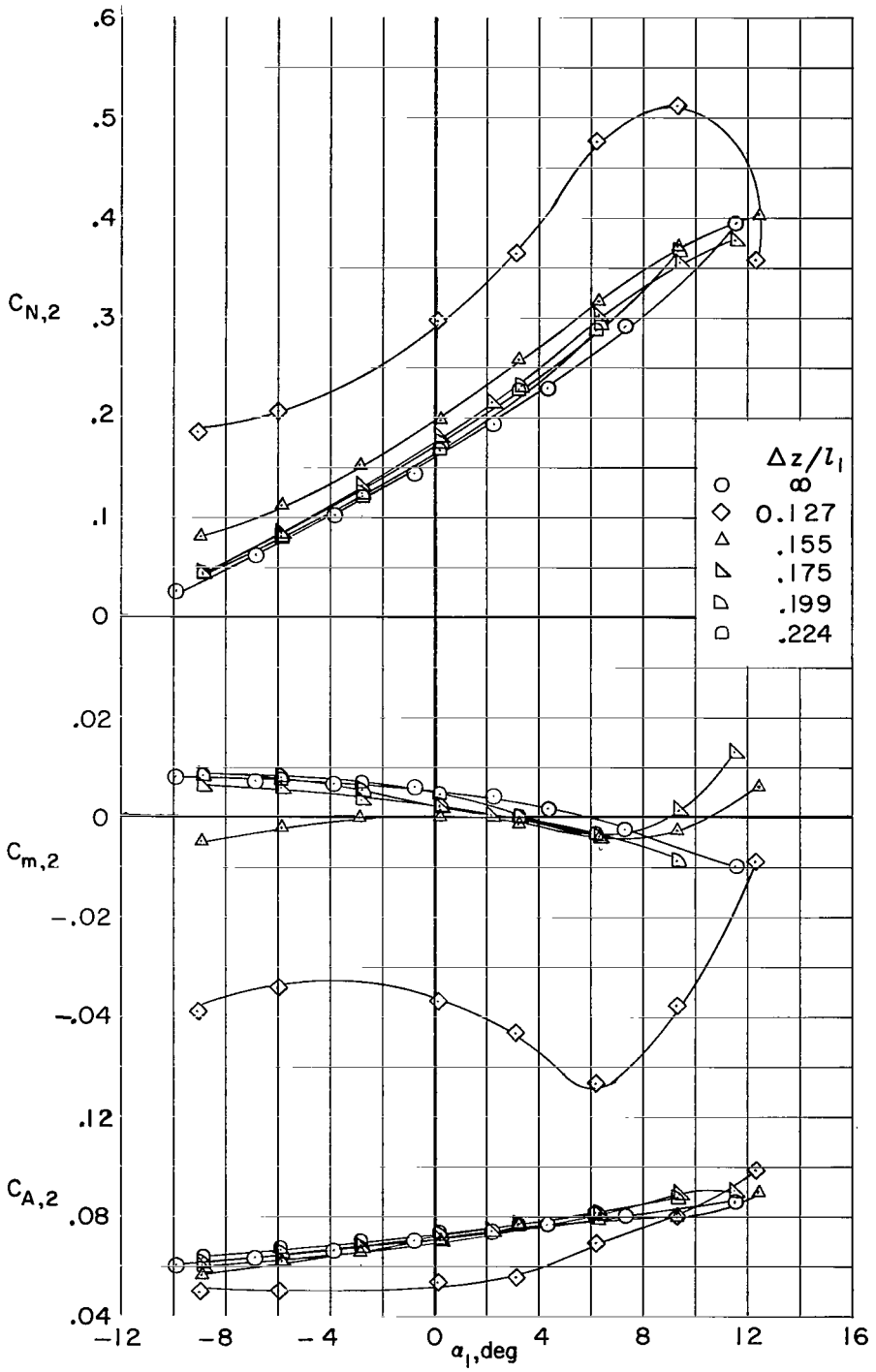

(f) $i = 10^0$; $\Delta x/l_1 = 0.160$.

Figure 9.- Concluded.

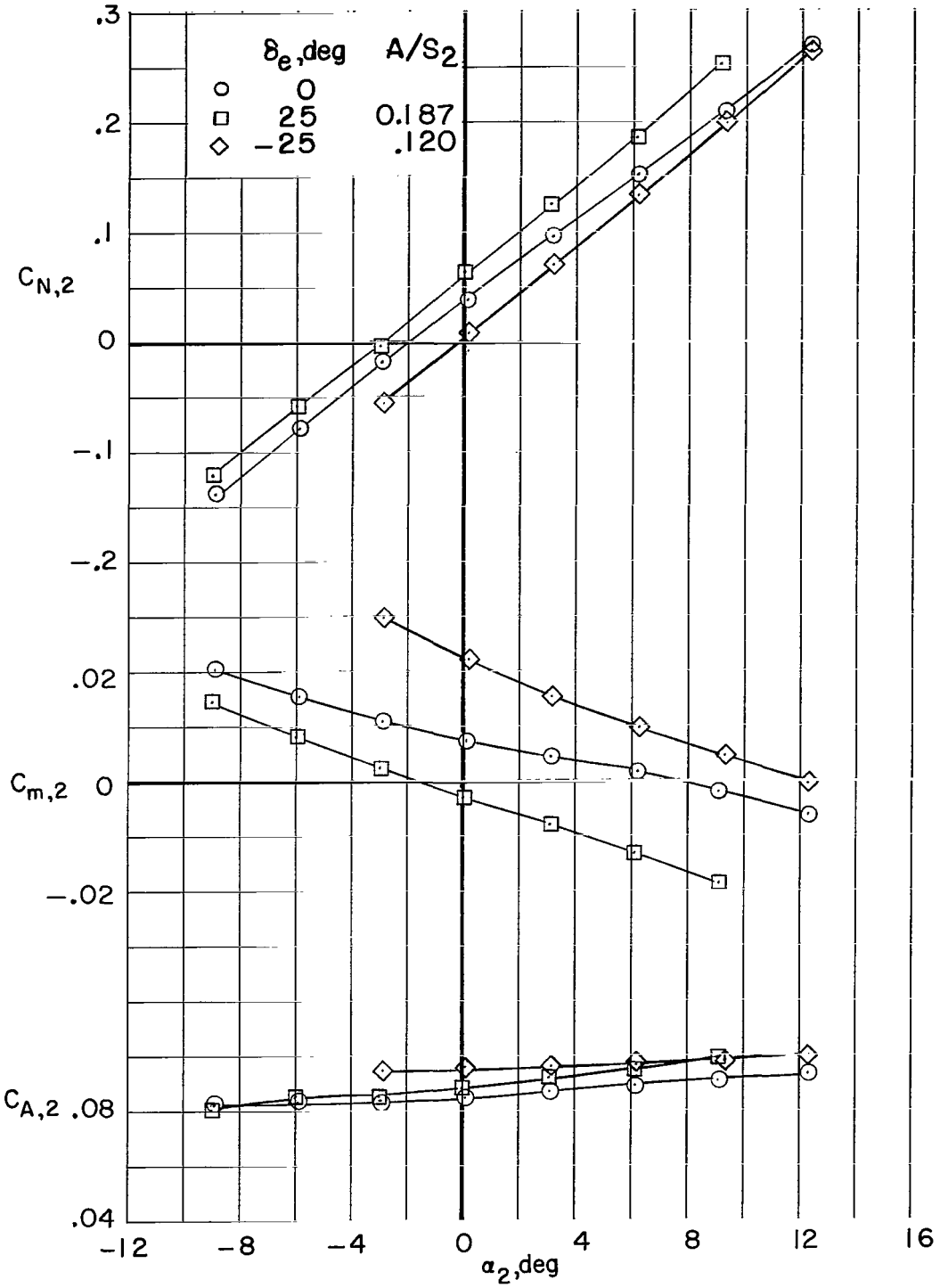

(a) M = 3.

Figure 10.- Control effectiveness for the second stage at interference free conditions.

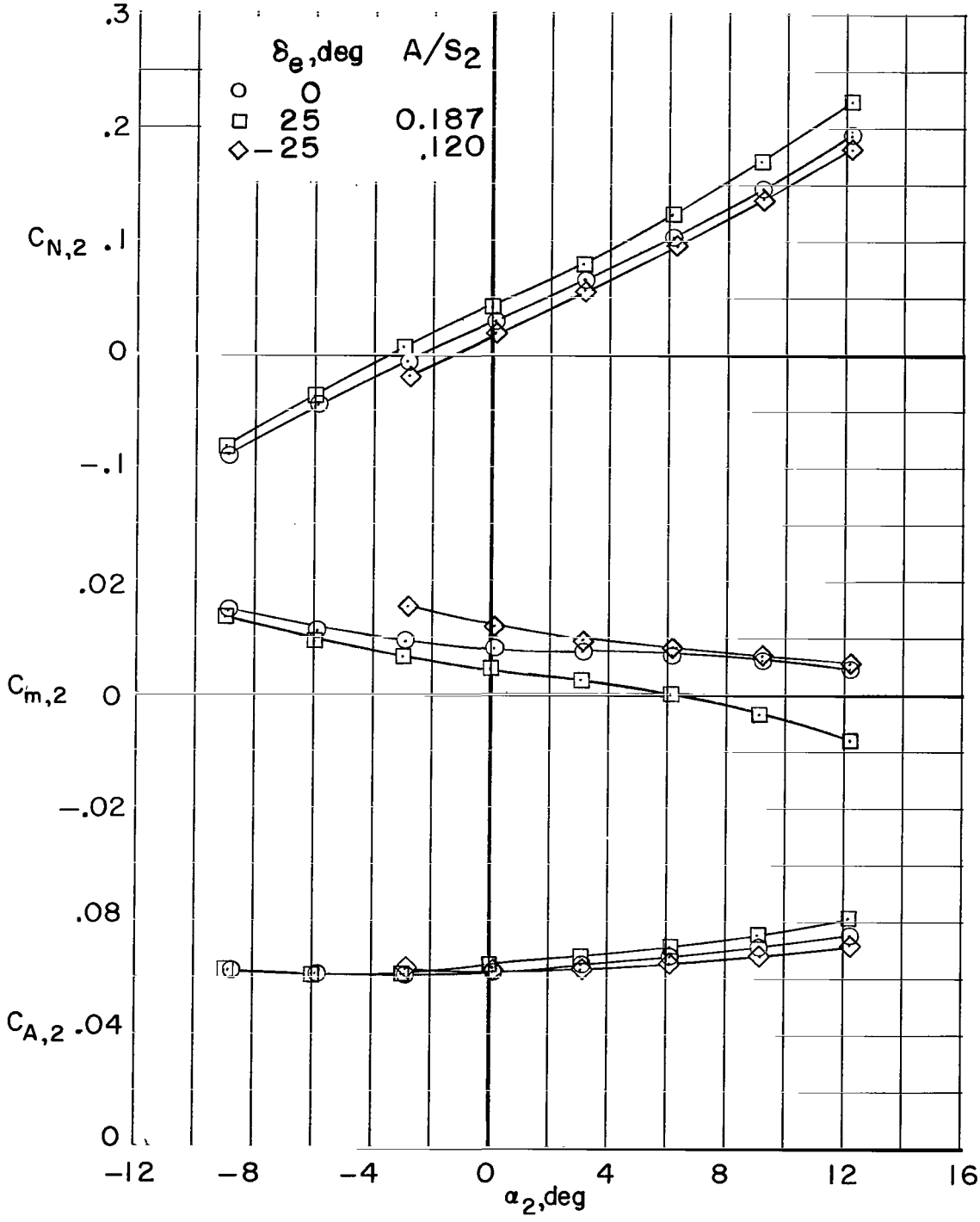

(b) M = 6.

Figure 10.- Concluded.

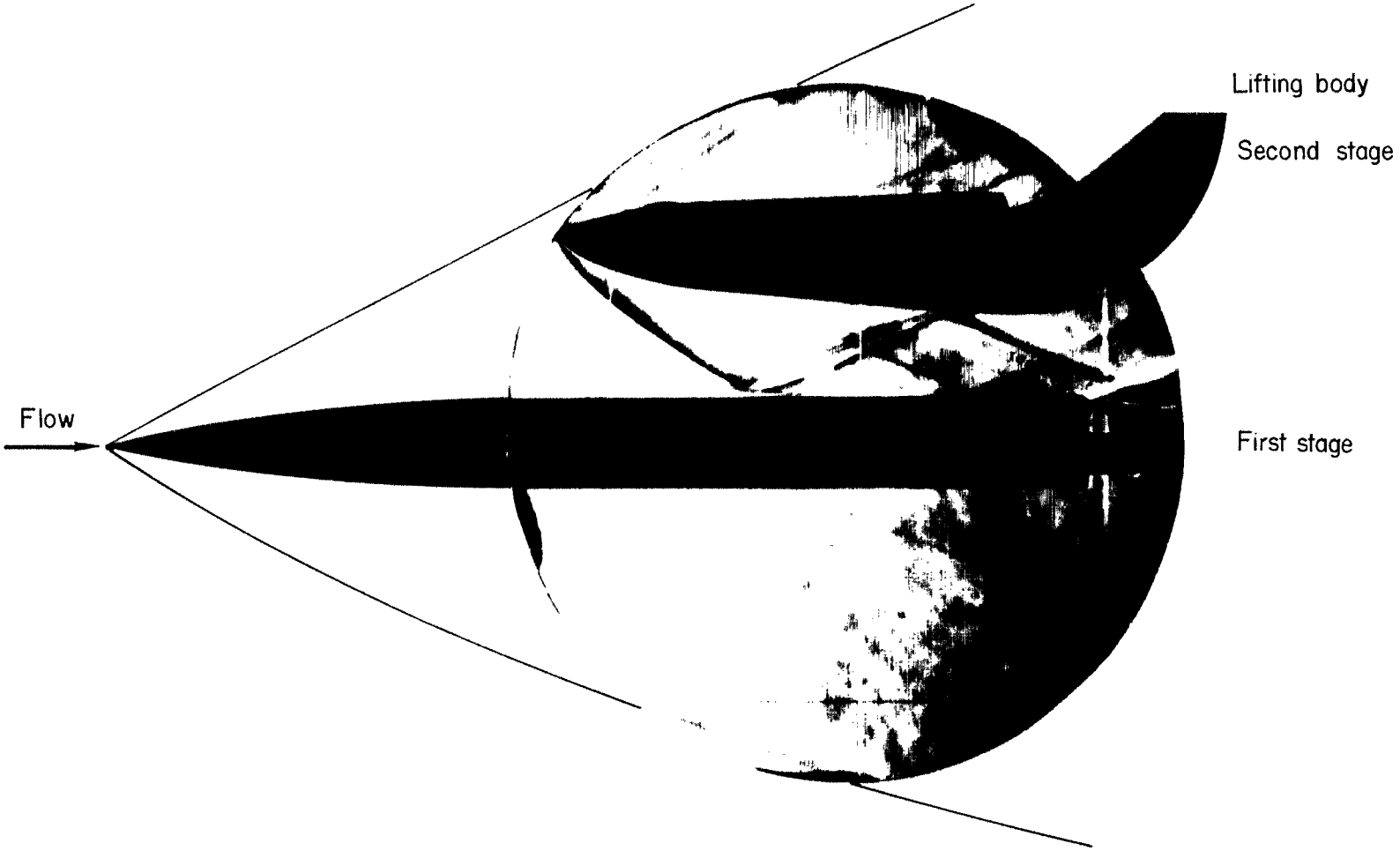

Figure 11.- Schlieren data. $M = 3$; $\alpha_1 = 0^0$; $i = 0^0$; $\Delta z/l_1 = 0.199$; $\Delta x/l_1 = -0.051$.

L-2866-7

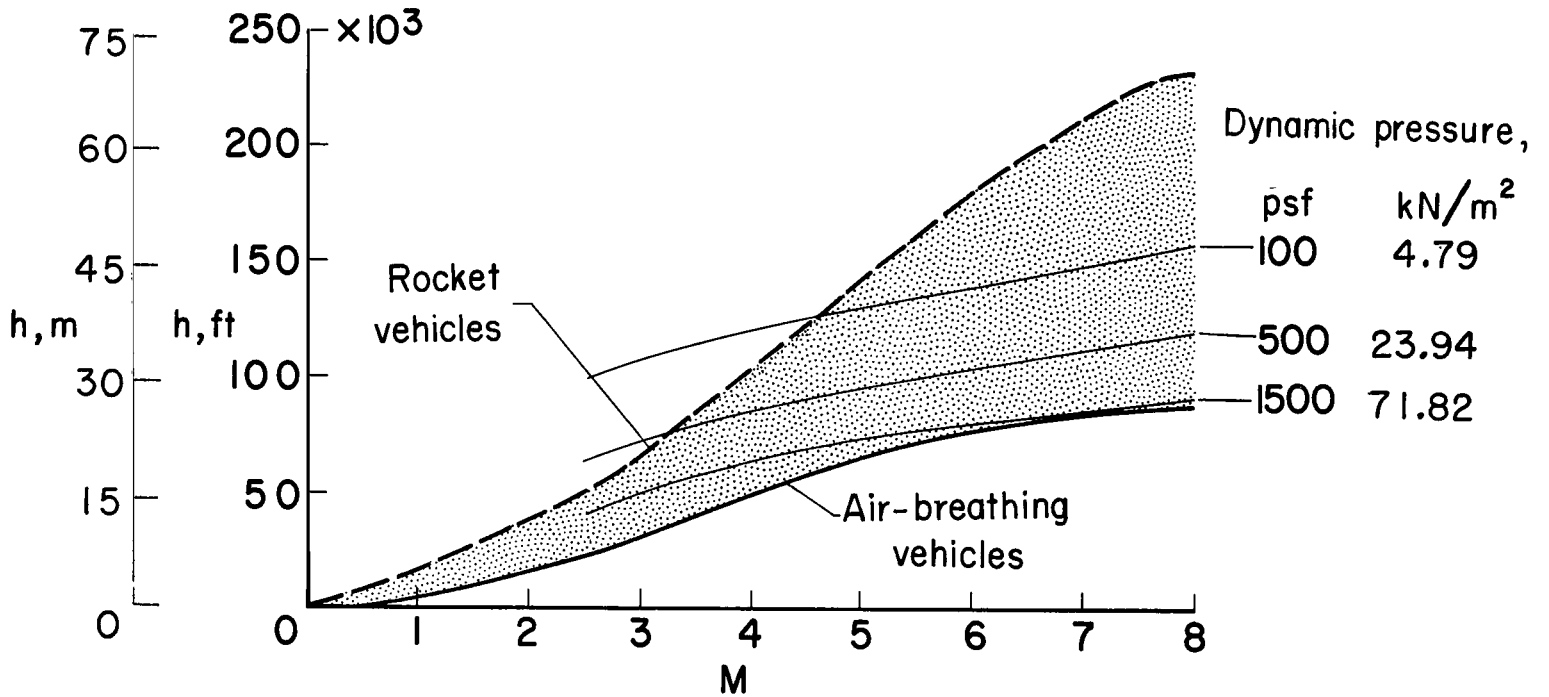

Figure 12.- Staging conditions.

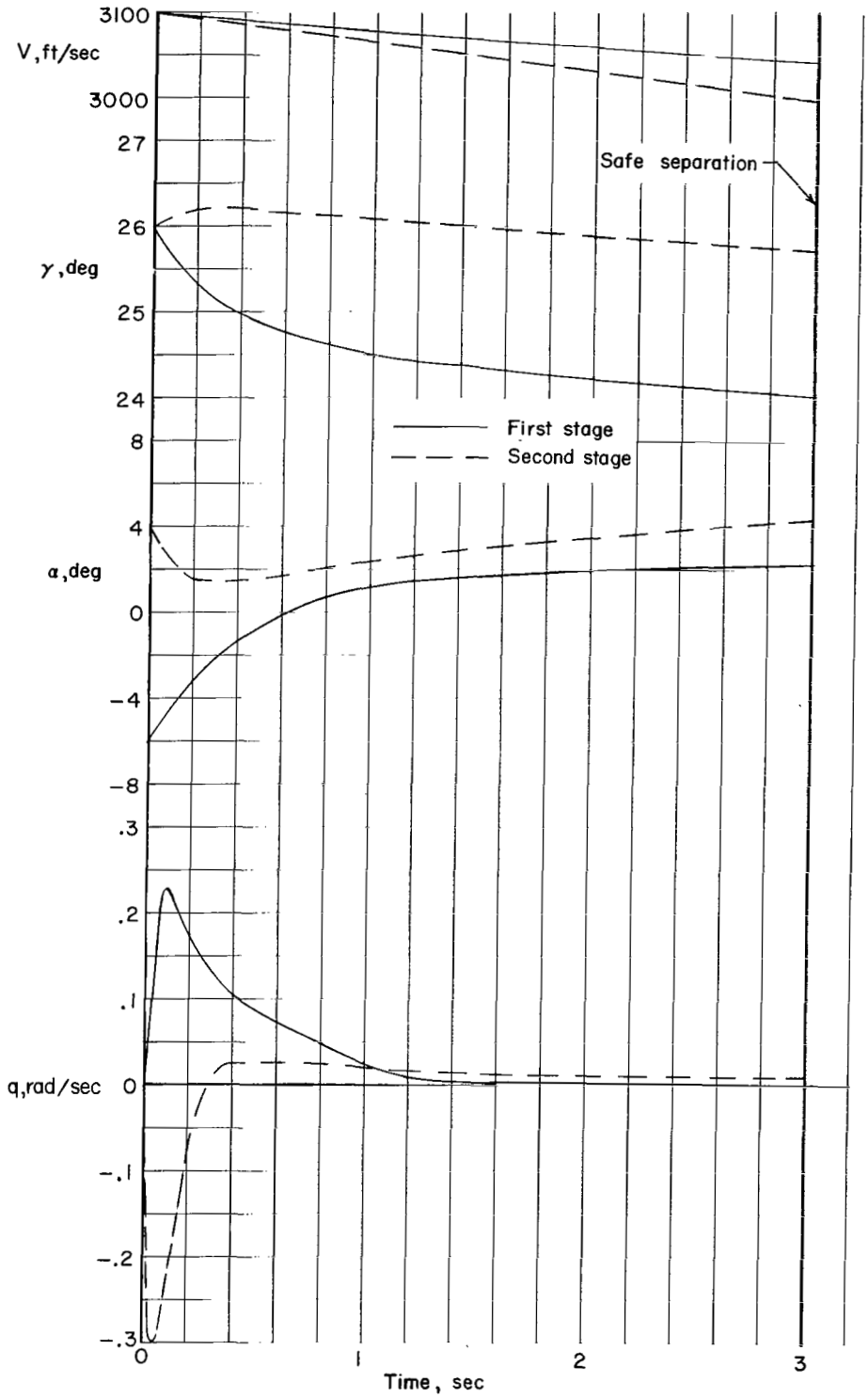

(a) Safe separation case. M = 3; h = 70 000 ft (21 336 m); $(C_{m_q})_1 = -40$ rad^{-1}; $(C_{m_q})_2 = -20$ rad^{-1}.

Figure 13.- Typical results from trajectory analysis.

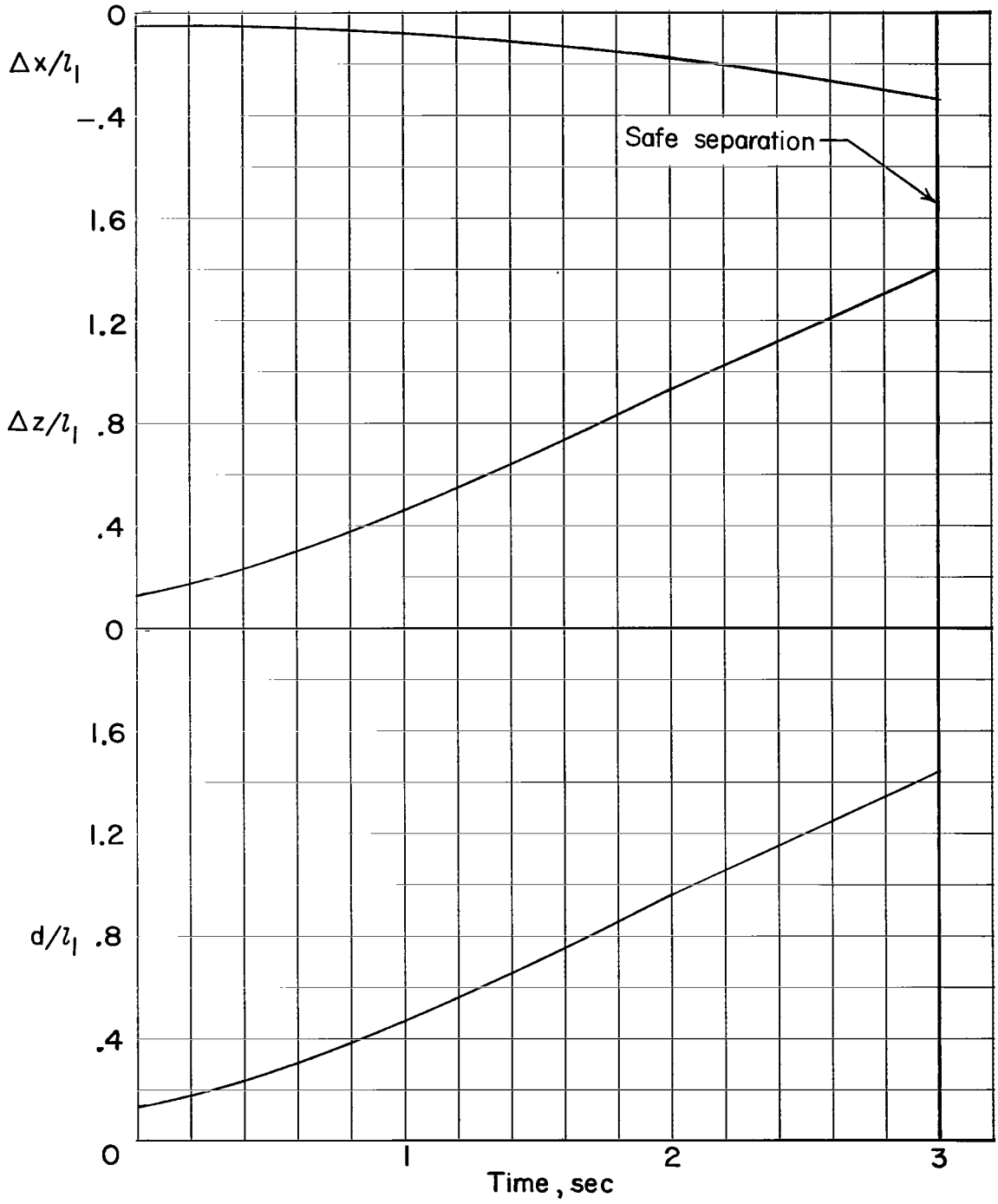

(a) Concluded.

Figure 13.- Continued.

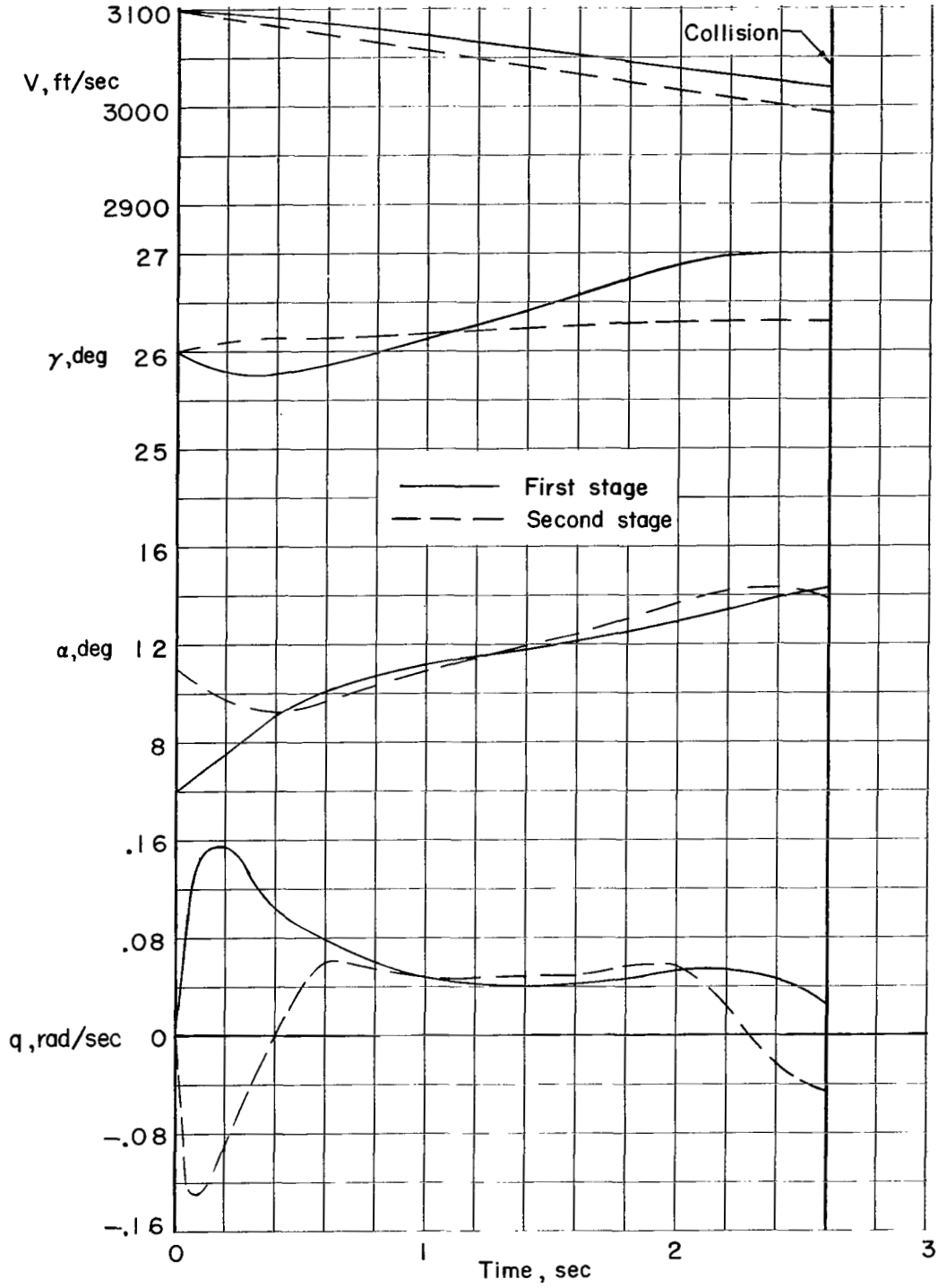

(b) Collision case. M = 3; h = 70 000 ft (21 336 m); $(C_{m_q})_1 = -20$ rad^{-1}; $(C_{m_q})_2 = -10$ rad^{-1}.

Figure 13.- Continued.

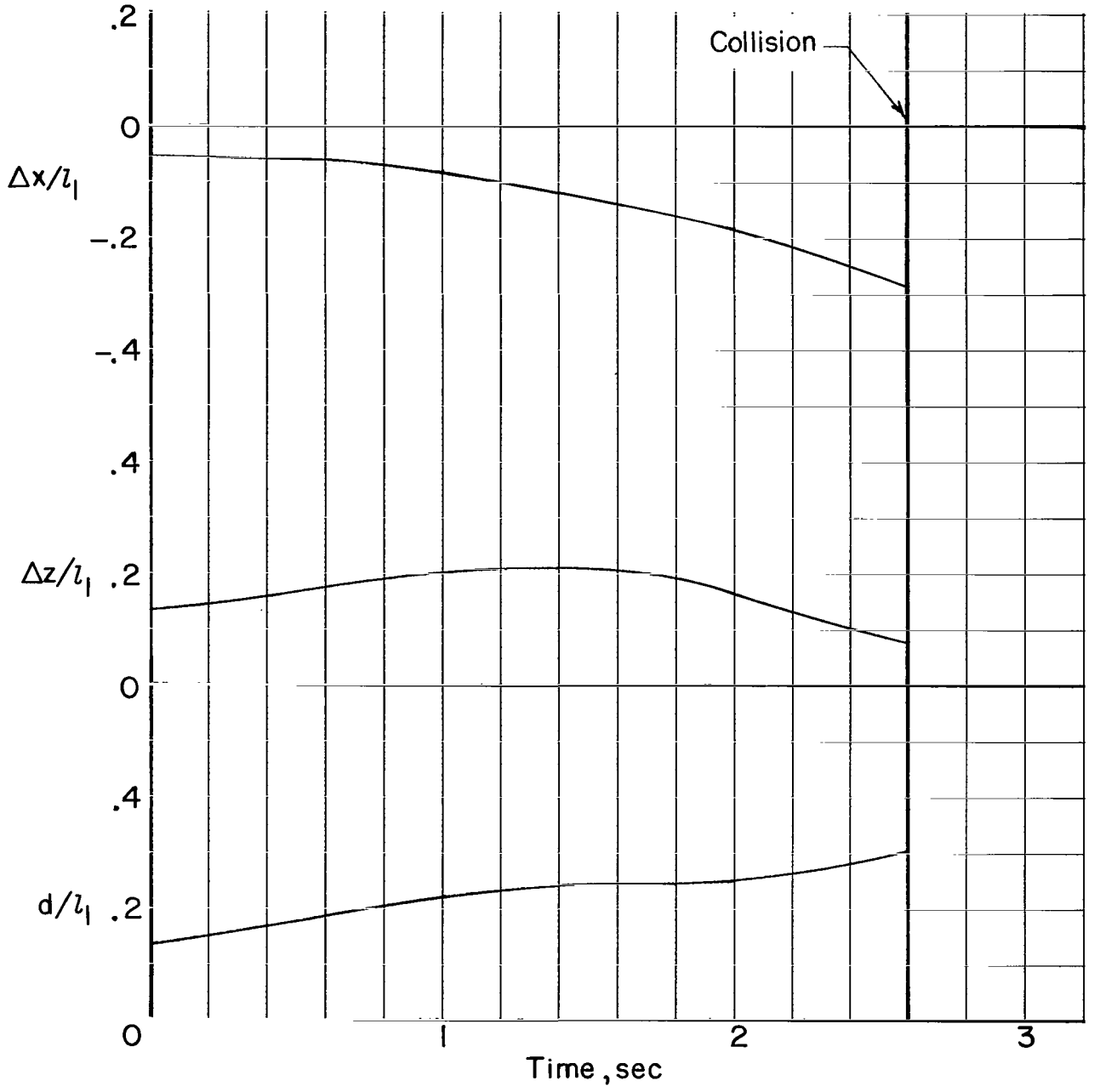

(b) Concluded.

Figure 13.- Concluded.

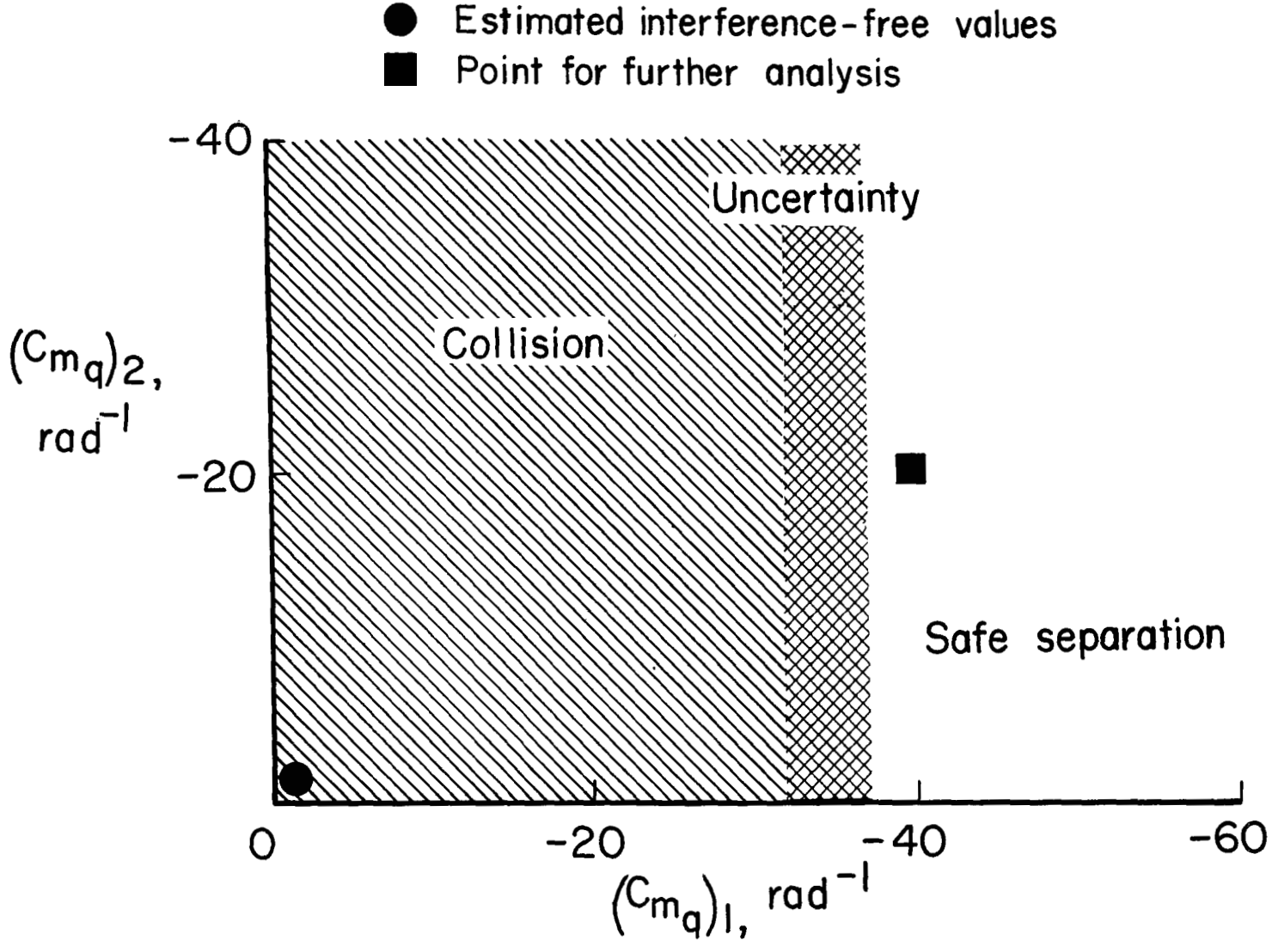

Figure 14.- Effect of dynamic derivatives on separation maneuver. M = 3; h = 70 000 ft (21 336 m); $\alpha_1 = 6^0$; $i = 5^0$.

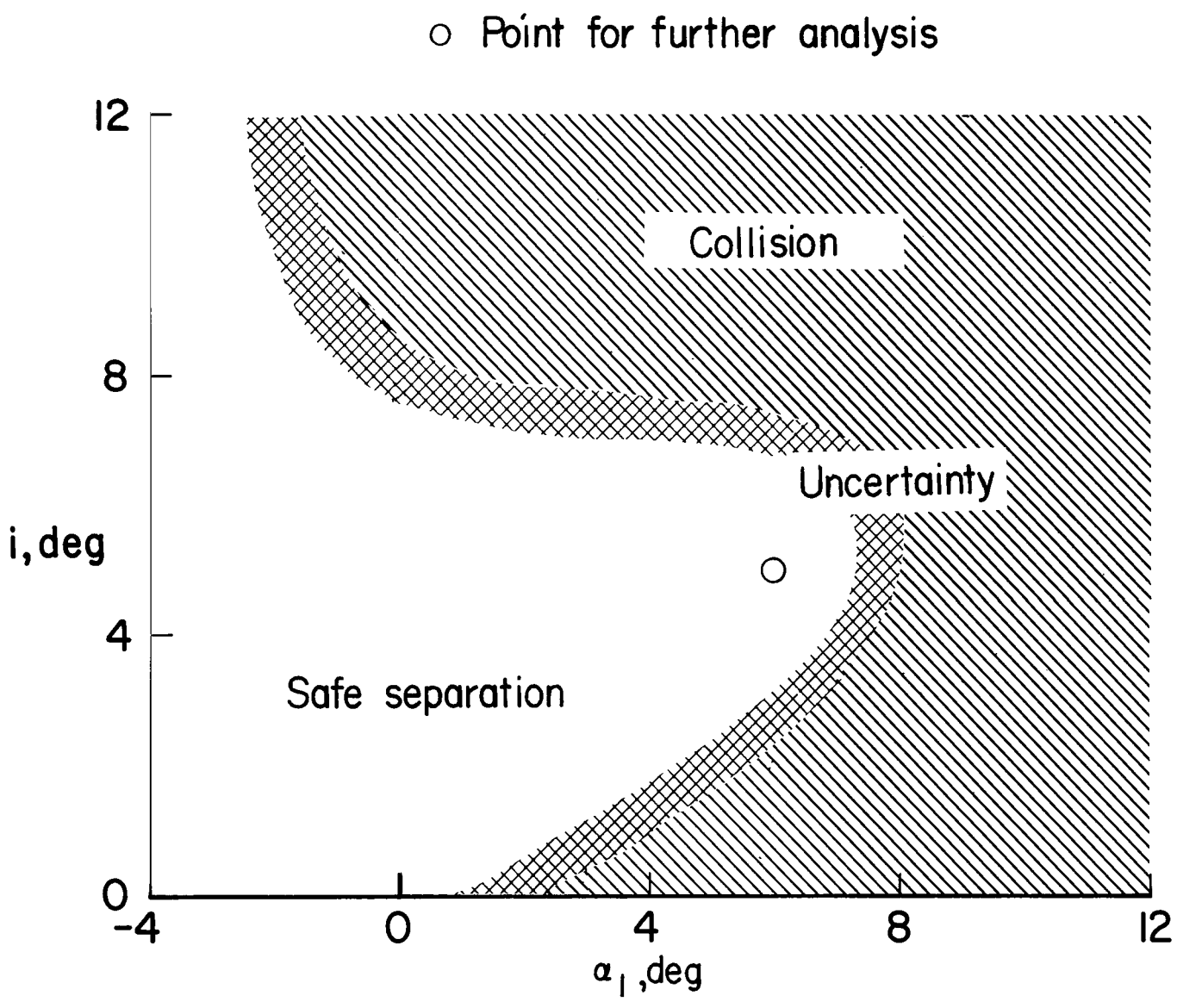

Figure 15.- Effect of initial attitude on separation maneuver. M = 3; h = 70 000 ft (21 336 m); $(C_{m_q})_1 = -40$ rad^{-1}; $(C_{m_q})_2 = -20$ rad^{-1}.

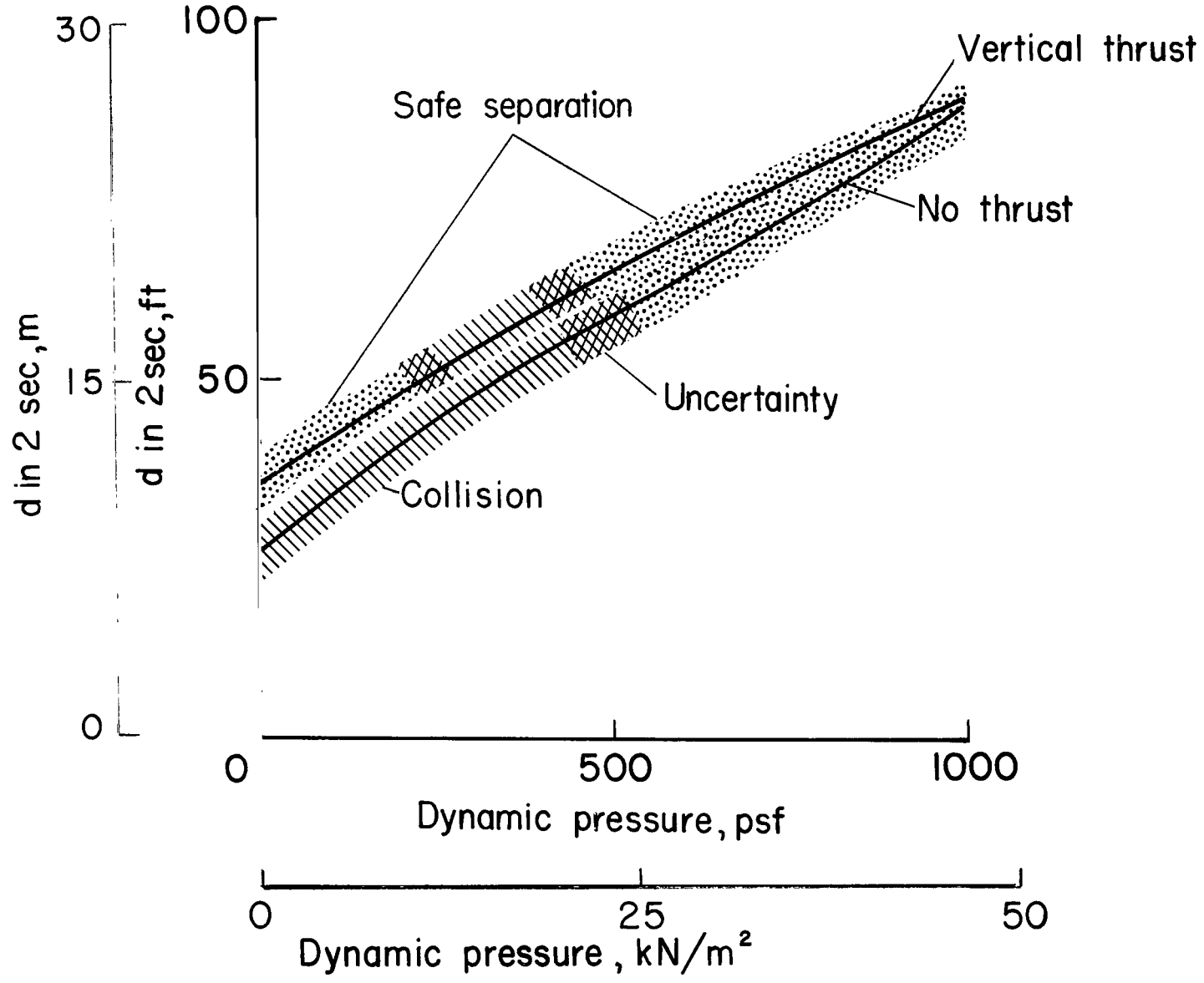

Figure 16.- Effect of dynamic pressure on separation maneuver. $M = 3$; $\alpha_1 = 6^0$; $i = 5^0$; $(C_{m_q})_1 = -40$ rad^{-1}; $(C_{m_q})_2 = -20$ rad^{-1}.

NATIONAL AERONAUTICS AND SPACE ADMINISTRATION
WASHINGTON, D. C. 20546

OFFICIAL BUSINESS

FIRST CLASS MAIL

POSTAGE AND FEES PAID
NATIONAL AERONAUTICS AND
SPACE ADMINISTRATION

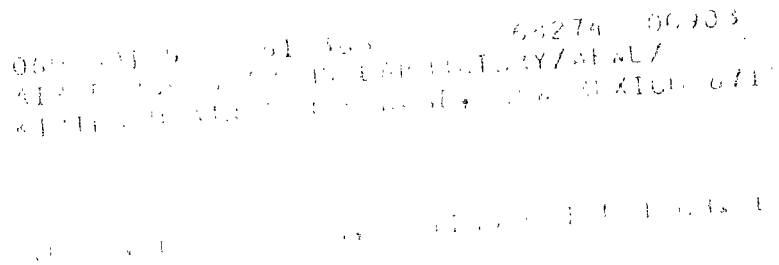

POSTMASTER: If Undeliverable (Section 158 Postal Manual) Do Not Return

"The aeronautical and space activities of the United States shall be conducted so as to contribute . . . to the expansion of human knowledge of phenomena in the atmosphere and space. The Administration shall provide for the widest practicable and appropriate dissemination of information concerning its activities and the results thereof."

—NATIONAL AERONAUTICS AND SPACE ACT OF 1958

NASA SCIENTIFIC AND TECHNICAL PUBLICATIONS

TECHNICAL REPORTS: Scientific and technical information considered important, complete, and a lasting contribution to existing knowledge.

TECHNICAL NOTES: Information less broad in scope but nevertheless of importance as a contribution to existing knowledge.

TECHNICAL MEMORANDUMS: Information receiving limited distribution because of preliminary data, security classification, or other reasons.

CONTRACTOR REPORTS: Scientific and technical information generated under a NASA contract or grant and considered an important contribution to existing knowledge.

TECHNICAL TRANSLATIONS: Information published in a foreign language considered to merit NASA distribution in English.

SPECIAL PUBLICATIONS: Information derived from or of value to NASA activities. Publications include conference proceedings, monographs, data compilations, handbooks, sourcebooks, and special bibliographies.

TECHNOLOGY UTILIZATION PUBLICATIONS: Information on technology used by NASA that may be of particular interest in commercial and other non-aerospace applications. Publications include Tech Briefs, Technology Utilization Reports and Notes, and Technology Surveys.

Details on the availability of these publications may be obtained from:

SCIENTIFIC AND TECHNICAL INFORMATION DIVISION

NATIONAL AERONAUTICS AND SPACE ADMINISTRATION

Washington, D.C. 20546